General Disclaimer

One or more of the Following Statements may affect this Document

- This document has been reproduced from the best copy furnished by the organizational source. It is being released in the interest of making available as much information as possible.

- This document may contain data, which exceeds the sheet parameters. It was furnished in this condition by the organizational source and is the best copy available.

- This document may contain tone-on-tone or color graphs, charts and/or pictures, which have been reproduced in black and white.

- This document is paginated as submitted by the original source.

- Portions of this document are not fully legible due to the historical nature of some of the material. However, it is the best reproduction available from the original submission.

Produced by the NASA Center for Aerospace Information (CASI)

ERRATUM:

Page No.	
7	Title of Table 2: Should read ".....$ZnO-TiO_2$....."
40	Line 4: Should read "SRI-treated....."
47	Line 3, 2nd Para., Should read ".....1/T(°K)".
48	Figure 19: Ordinate should read "1000/T(°K)".
49	Line 18, 2nd Para., Should read "....Figure 19....."
50	Lines 5,13.18 of Para., 3.4 Should read "...Figure 19".
51	Lines 12 and 16 Should read "......Figure 19....."

(NASA-CR-143850) DEVELOPMENT OF SPACE STABLE THERMAL CONTROL COATINGS FOR USE ON LARGE SPACE VEHICLES Triannual Report, 1 Sep.-31 Dec. 1974 (IIT Research Inst.) 87 p HC $4.75 CSCL 11D G3/27

N75-24937

Unclas 24754



Contract No. NAS8-26791
Report No. IITRI-C6233-48
(Triannual Report)

DEVELOPMENT OF SPACE STABLE THERMAL CONTROL COATINGS FOR USE ON LARGE SPACE VEHICLES

National Aeronautics and Space Administration
George C. Marshall Space Flight Center
Huntsville, Alabama 35812

Prepared by

J.E. Gilligan and Y. Harada

of

IIT Research Institute
Technology Center
Chicago, Illinois 60616

Sept 1 through December 31, 1974

Funded under Codes: 124-09-31-0000-33-1-004-080-2510
114-03-51-0000-33-2-004-080-2510

February, 1975

FOREWORD

This is Report No. IITRI-C6233-48 (Triannual Report) of IITRI Project C6233, Contract No. NAS8-26791, entitled "Development of Space Stable Thermal Control Coatings for Use on Large Space Vehicles." This report covers the period from September 1 through December 31, 1974.

Major contributors to the program during this period include: Mr. J.E. Gilligan, Project Leader; Mr. Y. Harada and Mr. W. Logan, pigment manufacturing studies; Mr. F.O. Rogers, paint preparation; Messrs A. Lackland and J. Brzuskiewicz, Irradiation experiments and reflectance measurements; and Dr. A.M. Stake, general consultation and administrative management.

The work reported herein was performed under the technical direction of the Space Sciences Laboratory of the George C. Marshall Space Flight Center; Mr. Daniel W. Gates acted as the Project Manager.

This contract was funded under Codes 124-09-31-0000-33-1-004-080-2510 and 114-03-51-0000-33-2-004-080-2510.

Respectfully submitted,
IIT RESEARCH INSTITUTE

J.E. Gilligan
Group Leader-Thermal Control
Polymer Chemistry Research

APPROVED:

A.M. Stake
Manager
Polymer Chemistry Research

JEG:ge

ABSTRACT

The effort toward the development of a large scale manufacturing method for the production of a stable zinc orthotitanate pigment has been continuing. During this period primary emphasis has been placed on the comprehensive analysis of the properties and environmental stability of oxalate precursor zinc orthotitanate pigments and of the preparative conditions (time and temperature) leading to optimum properties and optical stability.

TABLE OF CONTENTS

		Page
	FOREWORD	ii
	ABSTRACT	iii
1.	INTRODUCTION	1
2.	PIGMENT MANUFACTURING DEVELOPMENT STUDIES	2
	2.1 Particle Size Studies	2
	2.2 Coprecipitated Materials	2
	2.3 Stoichiometry Studies	6
	2.3.1 X-Ray Analyses	6
	2.3.2 Gravimetric Analyses	9
	2.3.3 SEM Analyses	11
	2.3.4 Optical Analysis	16
	2.3.5 Summary	24
	2.4 Ball-Milling Experiments	26
	2.4.1 SEM Investigations	26
	2.4.2 Optical Investigations	33
	2.5 Evaluation of SRI Treated Pigments-Sprayability	33
3.	CHARACTERIZATION OF OXALATE PRECURSORS	41
	3.1 Background	41
	3.2 Process Chemistry	41
	3.3 Oxalate Molecular Weight Determinations	42
	3.3.1 Zinc Oxalate	42
	3.3.2 "TiOx" Molecular Weight	43
	3.4 "TiOx" Characterization	50
	3.5 Conclusions	52
	APPENDIX I	53
	APPENDIX II	55
	APPENDIX III	57

TABLE OF CONTENTS (Cont'd)

		Page
4.	COMPHRENESIVE REVIEW	63
	4.1 Introductory Remarks	63
	4.2 Indices of Performance	63
	4.3 Analyses	67
	4.4 Conclusions	67
5.	REFERENCES	78

LIST OF TABLES

Table No.		Page
1	PARTICLE SIZE DETERMINATION OF Zn_2TiO_4 PIGMENTS	3
1A	PIGMENTS PREPARED FROM COPRECIPITATED (COP) OXALATE PRECURSORS	3
1B	PIGMENTS PREPARED FROM MIXTURES OF SEPARATELY PRECIPITATED OXALATE ("MOX") PRECURSORS	3
2	EFFECT OF STOICHIOMETRY ON PROPERTIES OF $ZnO:TiO_2$ MATERIALS	7
3	MOX PIGMENT STOICHIOMETRY SERIES RESULTS	22
4	BALL-MILLED Zn_2TiO_4 PIGMENT DATA	36
5	OBSERVATIONS OF SPRAYABILITY	37
6	BEHAVIOR OF SRI POWDERS	38
7	MASS LOSS DATA STATIC CALCINATION DATA	45
8	TGA DATA	46
9	CRITICAL PROPERTY/PERFORMANCE RELATIONSHIPS	65
10	COMPREHENSIVE LISTING OF ZINC ORTHOTITANATE PIGMENTS AND PAINTS	69
10A	1400°C PIGMENTS (AND THEIR PAINTS)	70
10B	1300°C PIGMENTS (AND THEIR PAINTS)	70
10C	1250°C PIGMENTS	71
10D	1200°C PIGMENTS (AND THEIR PAINTS)	71
10E	1100°C PIGMENTS	75
10F	1050°C PIGMENTS	75
10G	900°C PIGMENTS (AND THEIR PAINTS)	76

LIST OF FIGURES

Figure No.		Page
1	WEIGHT LOSS VS STOICHIOMETRY OF PRE-CALCINED PIGMENTS	10
2	SEM VIEWS OF MOX STOICHIOMETRY SAMPLES CALCINED AT 600°C/2 HRS.	12
3	SEM VIES OF MOX STOICHIOMETRY SAMPLES CALCINED AT 600°C/2 HRS.	13
4	SEM VIEWS OF MOX STOICHIOMETRY SAMPLES CALCINED AT 900°C/8 HRS.	14
5	SEM VIEWS OF MOX STOICHIOMETRY SAMPLES CALCINED AT 900°C/8 HRS.	15
6	SEM VIEWS OF MOX STOICHIOMETRY SAMPLES CALCINED AT 1200°C/2 HRS.	17
7	SEM VIEWS OF MOX STOICHIOMETRY SAMPLES CALCINED AT 1200°C/2 HRS.	18
8	REFLECTANCE SPECTRA OF 900°C MOX PIGMENTS WITH VARIOUS Zn/Ti MOLE RATIOS	19
9	REFLECTANCE SPECTRA OF 1200°C MOX PIGMENTS WITH VARIOUS Zn/Ti MOLE RATIOS	20
10	SEM VIEWS OF MOX-A AND MOX-A BALL MILLED	27
11	SEM VIEWS OF LH-105 AND LH-105 BALL MILLED	28
12	SEM VIEWS OF MOX-A AND MOX-A BALL MILLED, CALCINED AT 600°C/2 HRS.	29
13	SEM VIEWS OF LH-105 AND LH-105 BALL MILLED, CALCINED AT 600°C/2 HRS.	30
14	SEM VIEWS OF MOX-A AND MOX-A BALL MILLED, CALCINED AT 1200°C/2 HRS.	31
15	SEM VIEWS OF LH-105 AND LH-105 BALL MILLED, CALCINED AT 1200°C/2 HRS.	32

LIST OF FIGURES (Cont'd)

Figure No.		Page
16	REFLECTANCE SPECTRA OF LH-105(6-12) - BALL MILLED VS PLAIN	34
17	REFLECTANCE SPECTRA OF MOX-A(6-12) - BALL MILLED VS PLAIN	35
18	TGA THERMOGRAM OF "TiOx"	44
19	"TiOx" CONVERSION VS RECIPROCAL TEMPERATURE	48

Report No. IITRI-C6233-48
(Triannual Report)

DEVELOPMENT OF SPACE STABLE THERMAL CONTROL COATINGS FOR USE ON LARGE SPACE VEHICLES

1. INTRODUCTION

The effort in the research and development of passive spacecraft temperature control materials has, historically, concentrated on the development of the class of surfaces known as solar reflectors, surfaces with high reflectance for solar radiation and with high emittance in the thermal (infrared) spectrum. Basically, these surfaces must be optically stable in the total environment that they will experience. This requirement means that, once an high level of intrinsic stability in these materials is attained in the laboratory, we must make certain that this stability is preserved in a scaled-up process in manufacturing, that it is protected throughout the entire pre-launch environment, and, finally, that this stability obtains in the space environment. Applications on large space vehicles, therefore, present new R&D problems - not simply traditional ones in greater dimensions.

The program consists of four major tasks: pigment manufacturing development, binder development, environmental effects evaluations, and general coatings investigations. The relative emphasis on each of these tasks varies according to the urgency of the problems elucidated in our investigations, and, of course, with the availability of time and funds. Our present efforts have been expended primarily on the development of a pigment manufacturing method and related studies and on complementary environmental testing and evaluation activities.

2. PIGMENT MANUFACTURING DEVELOPMENT STUDIES

Studies were conducted in the following areas:

1. Determination of the particle size of Zn_2TiO_4 powders prepared during the course of the program.
2. Preparation of coprecipated Zn_2TiO_4 powders for use at Stanford Research Institute and at IITRI.
3. Evaluation of ball milling effects on optical properties of pigments.
4. Determination of effects of stoichiometry on compositional and optical properties.

These are discussed in the following sections.

2.1 Particle Size Studies

The particle sizes of Zn_2TiO_4 powders accumulated over the course of the program were analyzed. In general, the COP (coprecipitated) materials have shown good reproducibility in particle size whereas the MOX (mixed oxalate) samples have been somewhat inconsistent, attributable to the preliminary nature of the work. The particle size ranges determined from SEM studies are presented in Table 1.

2.2 Coprecipitated Materials

Approximately four pounds of Zn_2TiO_4 were produced by the COP method and forwarded to Stanford Research Institute for their study: 1200 grams of LH-111(6-12) to Mr. Eldon Farley, for plasma annealing studies, and 600 grams, to Dr. Kenneth Sancier for surface treatment experiments. The various steps in the processing of this material were as follows:

Table 1

Particle Size Determination of Zn_2TiO_4 Pigments

Table 1A

Pigments Prepared from Coprecipitated (COP) Oxalate Precursors

COP MATERIALS*	PARTICLE SIZE**	COMMENTS
As precipitated (un-calcined)	SM-5μ	Needle-like, as well as equiaxed shapes
(6):600°C/2 hrs	SM-5μ	Agglomeration caking effect
(6-9):600°C/2 hrs + 900°C/8 hrs	SM-5μ	Rounding of particles, less agglomeration than 600°C material
(6-10.5):600°C/2 hrs + 1050°C/2 hrs	1-5μ	Some necking between particles. No evidence of submicron material
(6-12):600°C/2 hr + 1200°C/2 hrs	2-5μ	Moderate necking, Rounded particles, no sharp edge effects
(6-14):600°C/2 hrs + 1400°C/2 hrs	2-5μ	Strong necking. Further rounding of particles.

*All Zn_2TiO_4 pigments from LH-16 to date. As indicated, the number in parenthesis denotes heat treatment. All pigments were pre-calcined at 600°C/2hrs. Good reproducibility from batch to batch permits this general analysis.

**SM = submicron

Table 1B

Pigments Prepared from Mixtures of Separately Precipitated Oxalate ("MOX") Precursors

MOX MATERIALS	PARTICLE SIZE	COMMENTS
Zinc oxalate precursor	2-5μ	
Titanium oxalate precursor	0.5-3μ	More irregularly shaped than ZnOx

Table 1B (Cont'd)

MOX MATERIALS - Cont'd	PARTICLE SIZE	COMMENTS - Cont'd
MOX,* as mixed (un-calcined)	0.5-4μ	
MOX(6)	SM-2 μ	Mostly submicron
MOX(6-10.5)	0.5-2μ	
MOX-A**	0.5-5μ	
MOX-A(6)	0.5-3μ	
MOX-A(6-9/4)†	1-3μ	
MOX-A(6-9/8)	1-3μ	
MOX-A(6-9/16)	1-3μ	Stronger necking than MOX-A(6-9/4), (6-9/8)
MOX-A(6-10.5/1)	1-4μ	
MOX-A(6-10.5/2)	1-4μ	Agglomeration
MOX-A(6-10.5/4)	1-4μ	
MOX-A(6-10.5/8)	1-4μ	
MOX-A(6-12/0.5)	1-5μ	
MOX-A(6-12/1)	1-5μ	Agglomeration and necking
MOX-A(6-12/2)	1-5μ	
MOX-B(6)***	0.5-3μ	
MOX-B(6-9/4)	SM-3μ	Agglomeration
MOX-B(6-9/16)	SM-3μ	
MOX-B(6-10.5/1)	1-5μ	
MOX-B(6-10.5/4)	1-5μ	Agglomeration and necking
MOX-B(6-10.5/8)	1-5μ	
MOX-B(6-12/0.5)	1-5μ	
MOX-B(6-12/2)	1-5μ	Strong necking

*MOX Composition is 2.05 Zn:1.00 Ti
**MOX-A Composition is 1.5 Zn:1.0 Ti
***MOX-B Composition is 2.05 Zn:1.00 Ti

†The number after the slash, e.g., the 4 in MOX-B(6-9/4), denotes the number of hours at the particular calcination temperature, in this case, 4hrs at 900°C after a pre-calcination at 600°C/2hrs.

1. Precipitation- Mixed oxalates having a mol ratio of 2.05 Zn:1.00 Ti were precipitated in an aqueous medium by reaction between a $ZnCl_2$-$TiCl_4$ mixture with oxalic acid. This was conducted at 90°C over a 4-hour period.

2. Filtration and drying- The precipitate was filtered with repeated hot water washings until the pH of the filtrate was about 7. Drying of the powder was conducted at 90°C for 18 hours.

3. Precalcination- The dried powder was precalcined at 600°C for 2 hours to remove decomposition volatiles, i.e, CO, CO_2, and H_2O, and to achieve partial conversion to Zn_2TiO_4.

4. Calcination- The precalcined powder was then calcined at 1200°C for 2 hours by "flash" calcination, i.e., direct insertion of powder (in a fused quartz container) into a furnace at 1200°C, soaked for 2 hours, and removed from the furnace. The resultant powder was hand pulverized in a porcelain mortar and crucible to reduce the agglomerates.

The precipitate was prepared in four batches of approximately 1200 gms each, the capacity of the reaction vessel. These batches were designated as LH-107. LH-108, LH-109, and LH-110.

Precalcination (600°C) was conducted as two batches: LH-107 + LH-109, and LH-108 + LH-110. The final 1200°C calcination was performed in one large batch to produce about 2000 grams of Zn_2TiO_4 pigment. This was designated as LH-111(6-12).

A large batch precipitation of 1220 grams has also been made. This has been designated LH-112 and will be kept in reserve for future Zn_2TiO_4 preparation as needed.

2.3 Stoichiometry Studies

The effects of different stoichiometries in the ZnO-TiO_2 system upon the optical properties of samples fired at elevated temperatures have been investigated. The compositions studied are as follows:

DESIGNATION	MOL RATIO, ZnO/TiO_2	THEORETICAL COMPOSITION ASSUMING Zn_2TiO_4 FORMATION
MOX-C	0.5/1	$Zn_2TiO_4 + 3\ TiO_2$
MOX-D	1.0/1	$Zn_2TiO_4 + 1\ TiO_2$
MOX-E	1.5/1	$Zn_2TiO_4 + 0.33\ TiO_2$
MOX-F	2.0/1	Zn_2TiO_4
MOX-G	2.5/1	$Zn_2TiO_4 + 0.5\ ZnO$

All compositions were processed by ball-milling of the individually precipitated oxalates, and mixed according to the various proportions indicated. Samples were fired initially (precalcined) at 600°C for two hours, and half of each sample composition was subsequently flash calcined at 900°C for eight hours, and the other half at 1200°C for two hours. A summary of the evaluation studies is presented in Table 2.

2.3.1 X-Ray Analyses

X-ray diffraction techniques were used to determine the chemical composition of the various samples. As shown in Table 2 Zn_2TiO_4 was found to be the major phase in all samples calcined at 600°C and higher, while at 600°C zinc metatitanate ($ZnTiO_3$) was present in lesser amounts as a second phase. These findings indicate that the reaction favors the formation of the orthotitanate in spite of a zinc deficiency (as in MOX-C, MOX-D, and MOX-E). It has been reported (ref. 1) that formation of the hexagonal metatitanate is favored when the TiO_2 is of the rutile crystalline modification or at least easily

Table 2

Effect of Stoichiometry on Properties of $ZnO \cdot TiO_2$ Materials

Sample	Zn/Ti Ratio	X-Ray Analysis Zn_2TiO_4	$ZnTiO_3$	ZnO	TiO_2	% Weight Loss
MOX-C(6)[1]	0.5/1	MAJ-1	MAJ-2			
MOX-D(6)	1.0/1	MAJ-1	MIN-1			
MOX-E(6)	1.5/1	MAJ-1	MIN-2			
MOX-F(6)	2.0/1	MAJ-1 *	MIN-2	MAJ-2		
MOX-G(6)	2.5/1	MAJ-1	MIN-2	MAJ-2		
MOX-C(9)[2]	0.5/1	MAJ-1		MIN-2	MIN-1	0.91
MOX-D(9)	1.0/1	MAJ-1 *	MIN-1		MIN-2	0.69
MOX-E(9)	1.5/1	MAJ-1 *				0.20
MOX-F(9)	2.0/1	MAJ-1 *				0.23
MOX-G(9)	2.5/1	MAJ-1		MIN-1		0.42
MOX-C(12)[3]	0.5/1	MAJ-1			MIN-1	1.05
MOX-D(12)	1.0/1	MAJ-1			MIN-1	0.64
MOX-E(12)	1.5/1	MAJ-1 *				0.24
MOX-F(12)	2.0/1	MAJ-1 *				0.25
MOX-G(12)	2.5/1	MAJ-1		MIN-1		0.33

*Evidence of $Zn_2Ti_3O_8$ phase

CODE: MAJ-1 Major Phase 1
MAJ-2 Major Phase 2
MIN-1 Minor Phase 1
MIN-2 Minor Phase 2

Notes: 1.) This series was calcined at 600°C/2hr.
2.) This series was calcined at 600°C/2hr. and at 900°C/8hr.
3.) This series was calcined at 600°C/2hr. and at 1200°C/2hr.

C6233-48

converted to rutile. Our work with titanium oxalate, i.e., "TiOx", has shown that anatase is formed at about 300°C, and that this crystalline phase persists at temperatures at least up to 700°C. Therefore, the lack of X-ray indicated presence of the rutile modification may account for the suppression of zinc metatitanate ($ZnTiO_3$) formation in favor of Zn_2TiO_4.

A third compound reported (ref. 1) in the ZnO-TiO_2 system is zinc sesquititanate, $Zn_2Ti_3O_8$. This compound is a simple cubic phase having a lattice constant somewhat smaller than that for the face centered cubic Zn_2TiO_4 (9.359 Å vs 8.456 Å). The facts that both phases are cubic and that the lattice constants are only slightly different result in almost identical d-spacing lines in the powder patterns. However, a simple cubic crystal ($Zn_2Ti_3O_8$) will exhibit a greater number of x-ray lines than a face-centered cubic material as in the case of (Zn_2TiO_4). Such extra lines have been observed in the patterns of MOX-F(6), MOX-D(9) MOX-E(9), MOX-F(9), MOX-E(12), and MOX-F(12), indicating the probable existence of the $Zn_2Ti_3O_8$ phase in these materials. This is a qualitative and not a quantitative observation. The other materials in these studies have not yet been examined for the presence of $Zn_2Ti_3O_8$. This will be done in the near future.

The occurrence of $Zn_2Ti_3O_8$ in MOX-F(6), MOX-D(9), and MOX-E(9) would appear reasonable in that MOX-F(6) is not completely reacted, and MOX-D(9) and MOX-E(9) are zinc deficient compositions. However, MOX-F(9) and MOX-F(12) have Zn:Ti ratios of 2:1 so that the x-ray indication of $Zn_2Ti_3O_8$ along with a negative indication of ZnO (except in MOX-F(6)) is somewhat puzzling. In addition, it is reported (ref. 1) that $Zn_2Ti_3O_8$ is transformed to $Zn_2TiO_4 + TiO_2$ at 1000°C, and thus the indicated existence of $Zn_2Ti_3O_8$ in MOX-E(12) appears anomalous. Additional analysis is needed in order to answer the apparent inconsistencies.

A third phase, ZnO, was detected in two of the 600°C materials, MOX-F(6) and MOX-G(6). This may be expected, since, at 600°C/2hrs the reaction is not complete. The lack of any detectable TiO_2 may be due to its presence as extremely fine crystallites which would not be within the sensitivity range of the X-rays.

At 900°C, Zn_2TiO_4 is again the major phase in all samples - but with evidence of some $Zn_2Ti_3O_8$. The metatitanate, $ZnTiO_3$, was observed in only MOX-D(9), suggesting that conversion to the orthotitanate had occurred in the other samples. An important observation for the 900°C materials is that MOX-E(9) did not show any TiO_2 phase. Relative to Zn_2TiO_4 the 1.5 to 1 ratio of Zn to Ti for MOX-E would suggest an excess of TiO_2, but none was detected. A similar observation was made with MOX-A a similar composition reported previously in reference 2. As discussed later, this apparent absence of TiO_2 was reflected in the optical properties.

At 1200°C, MOX-C(12) and MOX-D(12) showed excess TiO_2 as would be expected from their zinc deficient compositions. As was the case at 900°C, the MOX-E and MOX-F samples showed Zn_2TiO_4. The zinc excess in the MOX-G composition showed up clearly as ZnO in the x-ray analysis.

2.3.2 Gravimetric Analyses

All samples calcined at 600°C displayed weight losses of 45 to 48%, corresponding to calculated theoretical decomposition losses. Weight changes were also determined for material calcined at 900° and 1200°C, and these data are shown in Table 2 and graphically presented in Figure 1.

The data show the highest weight loss, about 1%, for MOX-C material. A minimum can be observed for MOX-E and MOX-F

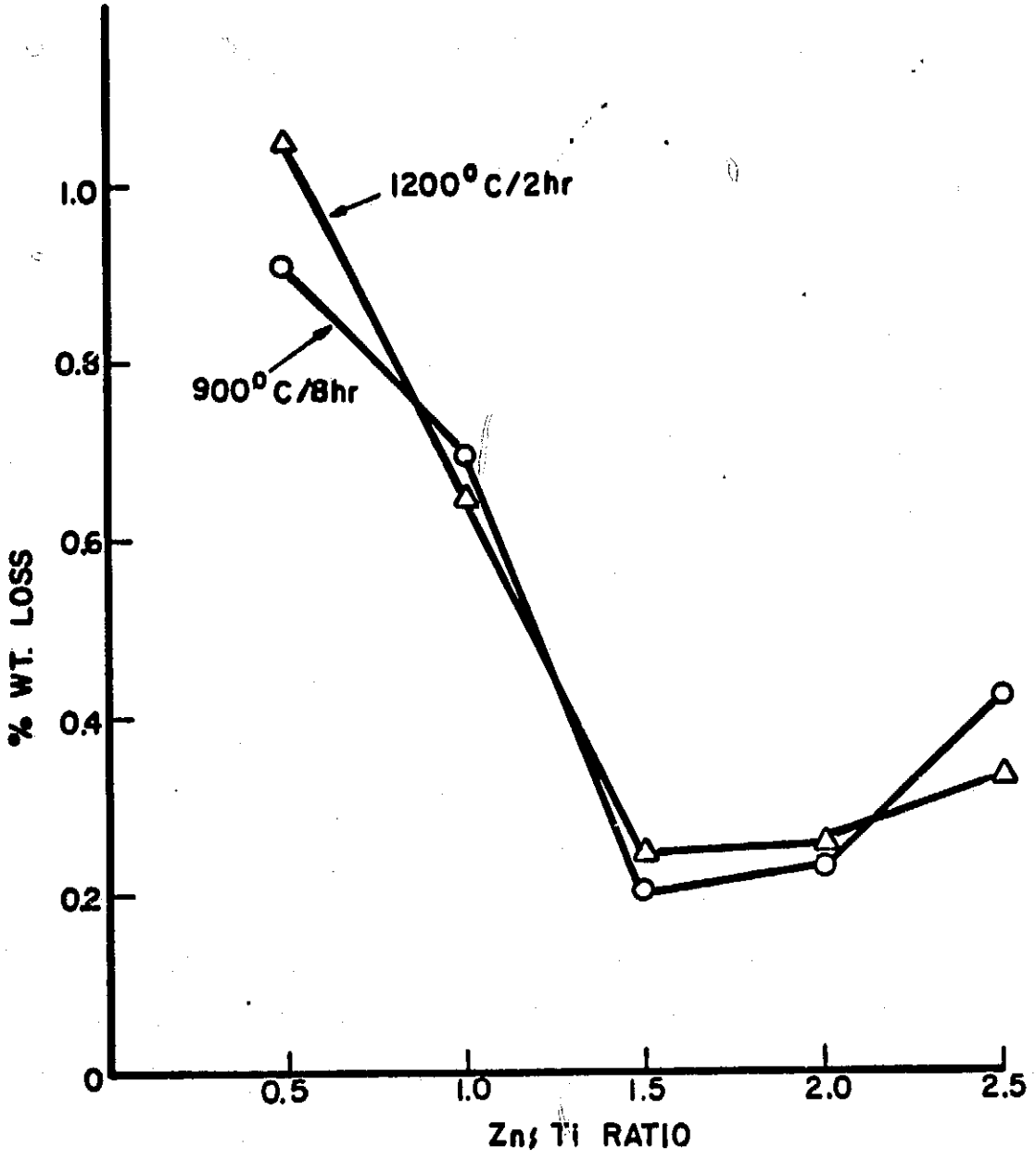


Fig. 1. WEIGHT LOSS VS STOICHIOMETRY OF PRE-CALCINED PIGMENTS

materials, and a slight increase for the excess zinc MOX-G samples. There does not appear to be a strong difference between losses at the two temperatures.

From the observed minimum, it appears that materials at or near the stoichiometry of Zn_2TiO_4 exhibit the smallest weight losses. The MOX-E and MOX-F samples also show a strong predominance of Zn_2TiO_4. The higher weight losses occur in those materials in which TiO_2 or ZnO was detected. Thus, weight loss appears related to completeness of reaction.

It should also be noted that the weight losses were quite small, indicating very limited volatility for either the excess TiO_2 or ZnO. It is somewhat puzzling, therefore, that the TiO_2 shows up as a very minor phase in X-ray analysis in MOX-C(12) and in MOX-D(12), and not at all in MOX-E(12) in which a 0.33 mol excess of TiO_2 should exist.

2.3.3 SEM Analyses

Materials calcined at the three temperature levels have been examined by D.W. Gates using SEM techniques. Preliminary examination of photographs have revealed the following:

At 600°C:

1. All samples heterogeneous, i.e., agglomerates and discrete particles with a range in particle size and shape.
2. A trend toward finer particles and less agglomeration with increasing Zn/Ti ratio. (See Figures 2 and 3).

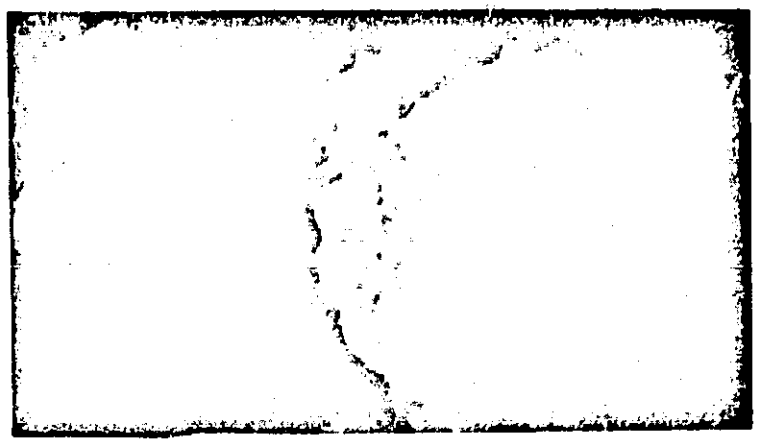
At 900°C:

1. Similar trend in particle size and state of agglomeration. MOX-G(9) appeared to have particularly fine particles.
2. All samples contained submicron particles. Largest particles were about 2μ. (See Figures 4 and 5).

10μ



581 MOX-C (6):0.5Zn/1Ti 3000X MOX-C



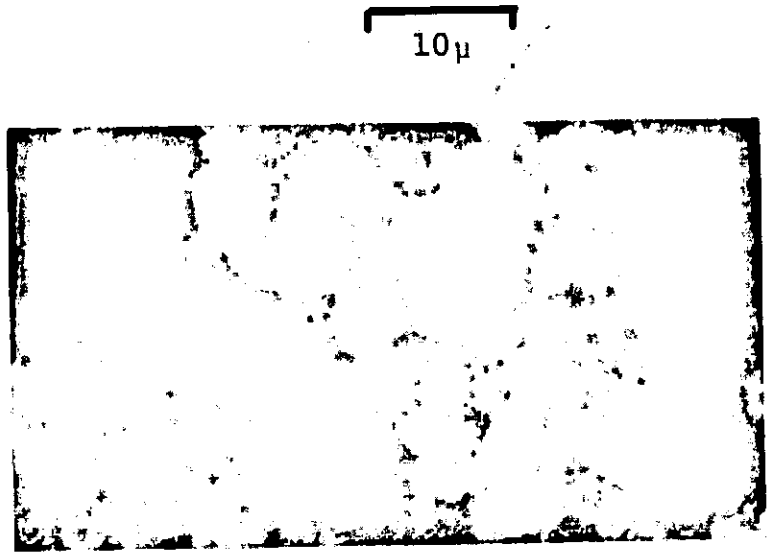
588 MOX-D (6):1Zn/1Ti 3000X MOX-D



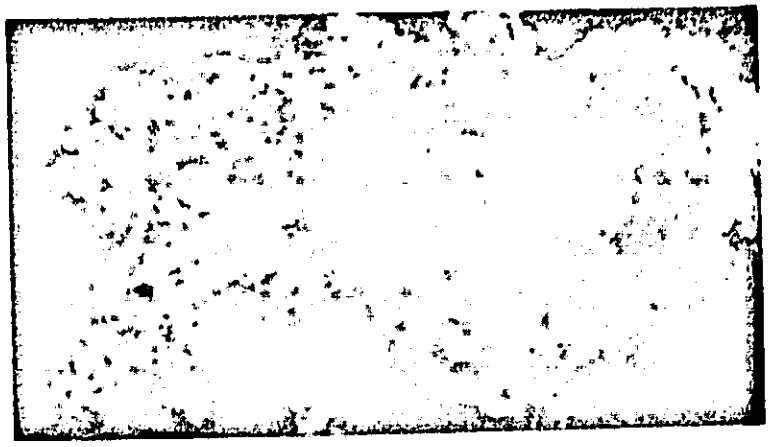
577 MOX-E (6):1.5Zn/1Ti 3000X MOX-E

Figure 2. SEM Views of MOX Stoichiometry Samples Calcined at 600°C/2 Hrs.

ORIGINAL PAGE IS
OF POOR QUALITY



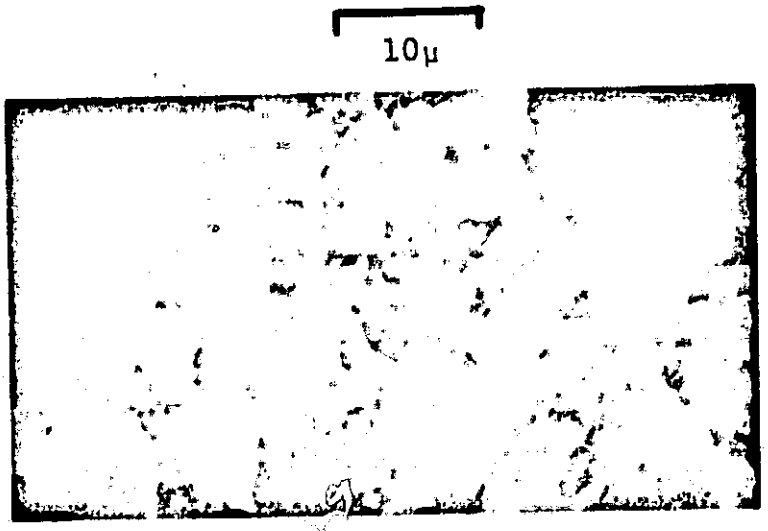
575 MOX-F(6):2Zn/1Ti 3000X MOX-F



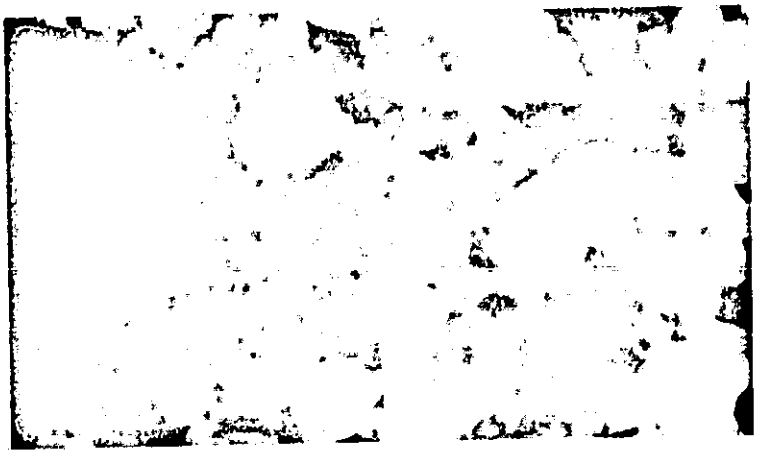
584 MOX-G(6):2.5Zn/1Ti 3000X MOX-G

Figure 3. SEM Views of MOX Stoichiometry Samples Calcined at 600°C/2 Hrs.

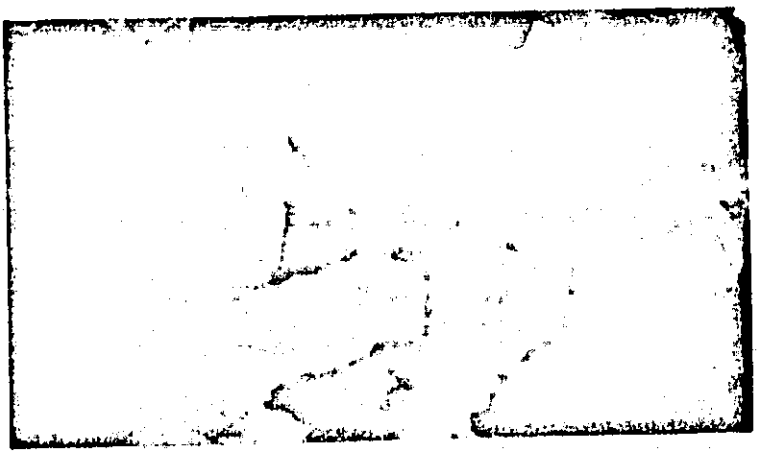
ORIGINAL PAGE IS
OF POOR QUALITY



587 MOX-C (9):0.5Zn/1Ti 3000X MOX-C



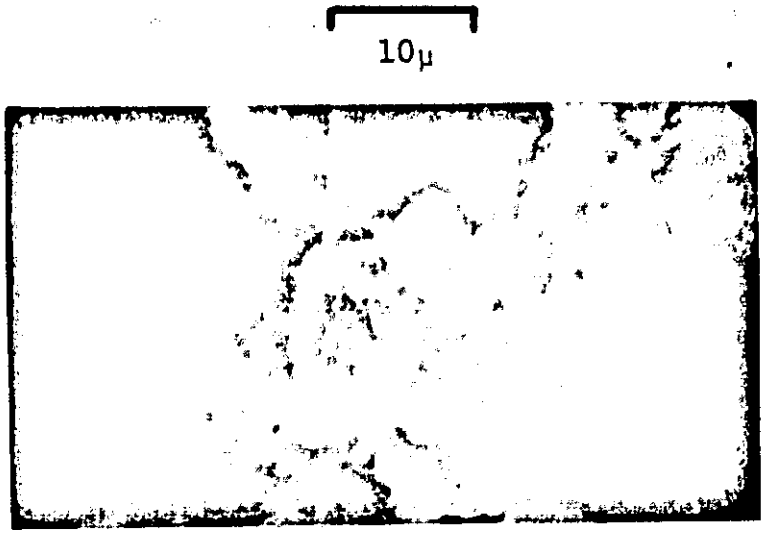
586 MOX-D (9):1Zn/1Ti 3000X MOX-D



582 MOX-E (9):1.5Zn/1Ti 3000X MOX-E

Figure 4. SEM Views of MOX Stoichiometry Samples Calcined at 900°C/8 Hrs.

ORIGINAL PAGE IS
OF POOR QUALITY



579 MOX-F(9):2Zn/1Ti 3000X MOX-F



578 MOX-G(9):2.5Zn/1Ti 3000X MOX-G

Figure 5. SEM Views of MOX Stoichiometry Samples Calcined at 900°C/8 Hrs.

ORIGINAL PAGE IS
OF POOR QUALITY

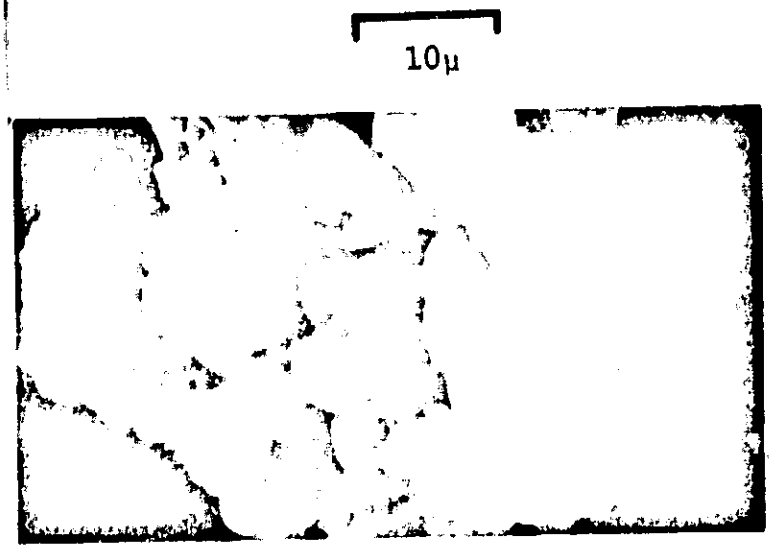
At 1200°C:

1. All samples showed necking and sintering of particles.
2. Particle size was significantly greater than for the 900°C samples. MOX-C(12) and MOX-D(12) contained some submicron particles. MOX-E(12), MOX-F(12), and MOX-G(12) were about 1-5μ.
3. MOX-C(12) and MOX-D(12) particles exhibited sharper edges, whereas the others all had rounded edges. The necking appeared weaker for MOX-C(12) and MOX-D(12) compared to the others. (See Figures 6 and 7).

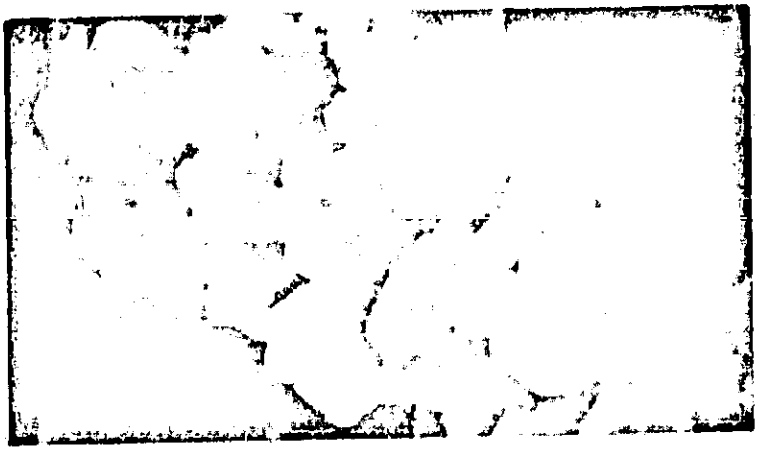
2.3.4 Optical Analysis

The diffuse reflectance spectra (320 to 500nm) for the 900°C and 1200°C samples of MOX-C thru MOX-G are exhibited in Figures 8 and 9. Also included is the curve for LH-106(6-12) which, judging from the band edge, evidently possesses exact Zn_2TiO_4 stiochiometry.

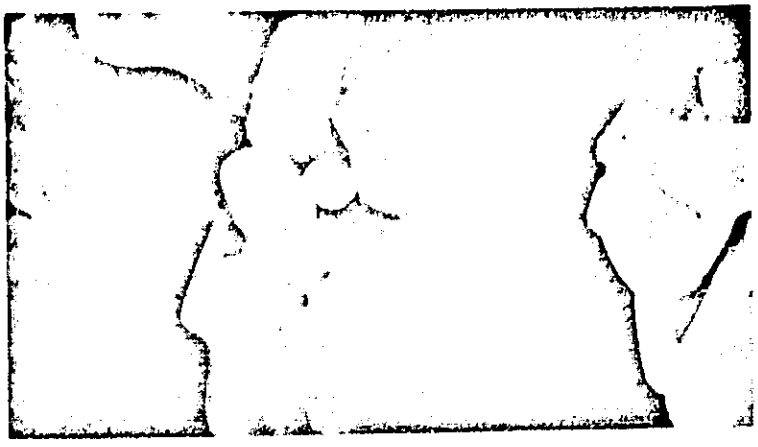
The spectra in Figs. 8 and 9 reveal some important similarities. In both cases, the band edge shifts with increasing Zn/Ti ratio toward shorter wavelengths until a pigment with a Zn excess is produced (MOX-G). The shapes of the band edges provide deeper insight. The MOX-G samples (2.5:1) show a "knee" which is much more flat than that exhibited by other samples; this is a characteristic signature of free ZnO. It reveals itself in this way because of its sharp fundamental absorption spectrum and its very intense absorption below 376nm. By contrast the fundamental electronic absorption spectrum for both rutile and anatase TiO_2 is more gentle, and it possesses an absorption constant approximately an order of magnitude less than that of ZnO (below 376nm). The curvature (the shape) of



580 MOX-C (12):0.5Zn/1Ti 3000X MOX-C



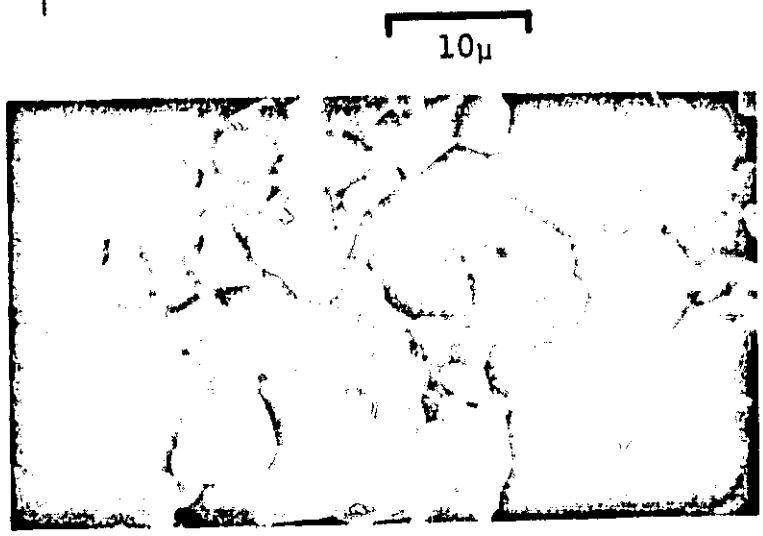
576 MOX-D (12):1Zn/1Ti 3000X MOX-D



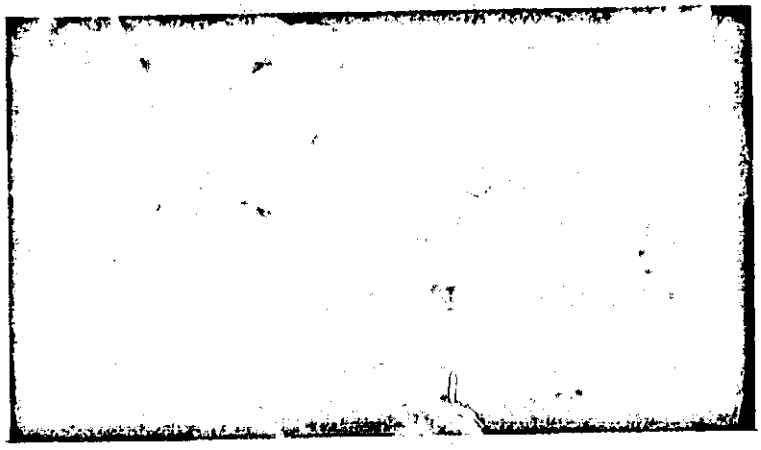
583 MOX-E (12):1.5Zn/1Ti 3000X MOX-E

Figure 6. SEM Views of MOX Stoichiometry Samples Calcined at 1200°C/2 Hrs.

ORIGINAL PAGE IS OF POOR QUALITY



585 MOX-F(12):2Zn/1Ti 3000X MOX-F



574 MOX-G(12):2.5Zn/1Ti 3000X MOX-G

Figure 7. SEM Views of MOX Stoichiometry Samples Calcined at 1200°C/2 Hrs.

ORIGINAL PAGE IS
OF POOR QUALITY

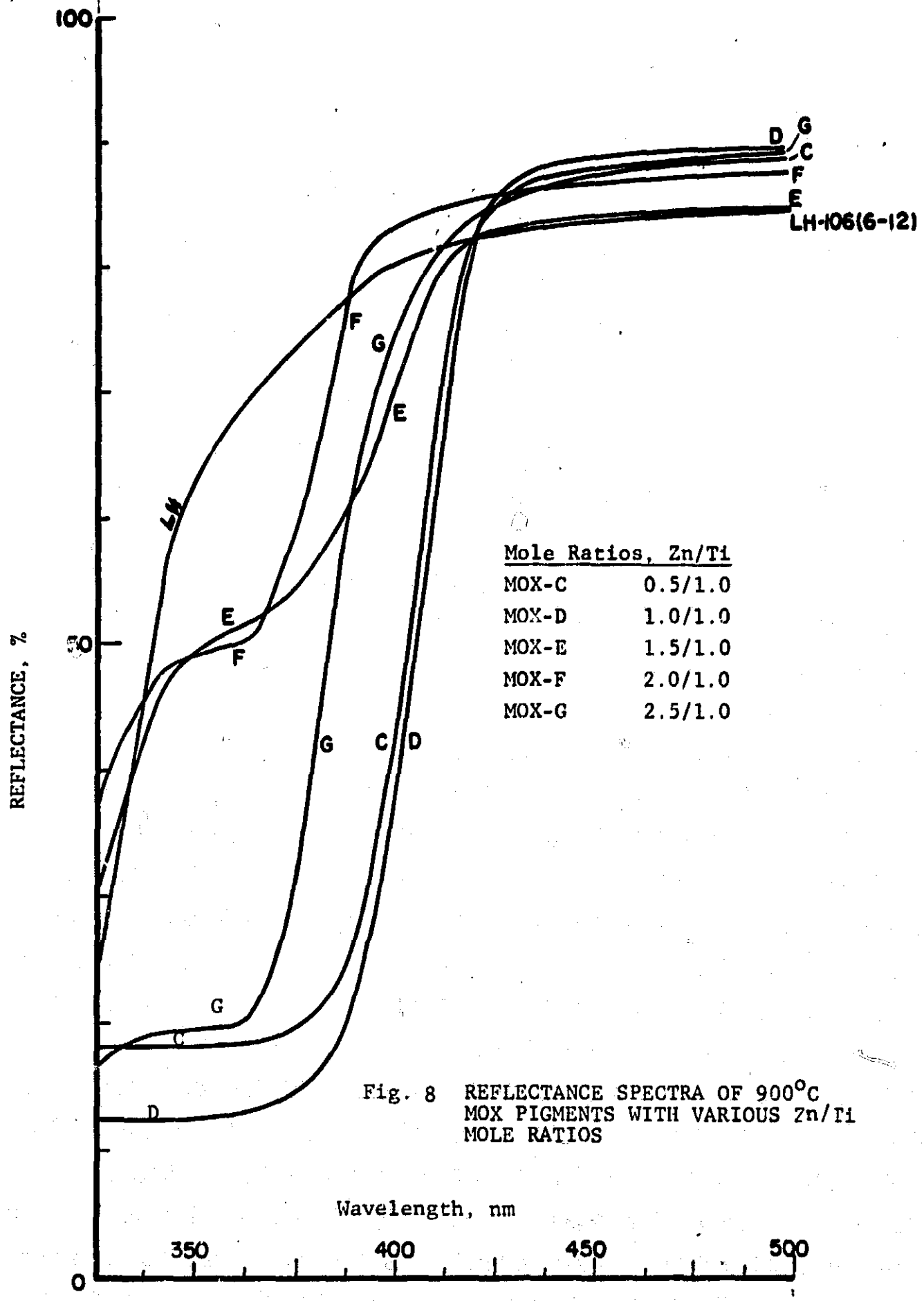


Fig. 8 REFLECTANCE SPECTRA OF 900°C MOX PIGMENTS WITH VARIOUS Zn/Ti MOLE RATIOS

C6233 -48

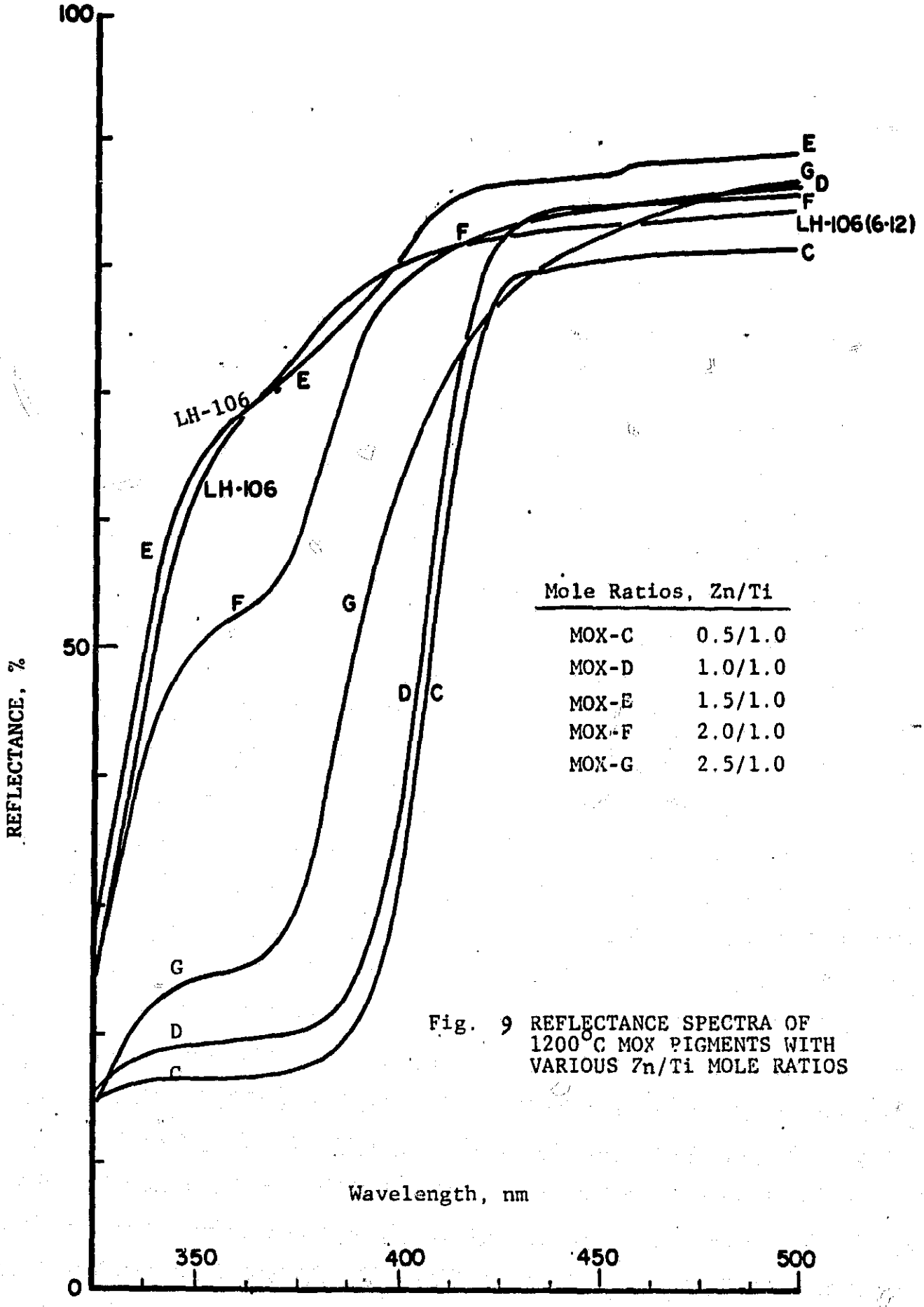


Fig. 9 REFLECTANCE SPECTRA OF 1200°C MOX PIGMENTS WITH VARIOUS Zn/Ti MOLE RATIOS

the knee for the Zn-deficient samples obviously is much greater than that in the Zn-rich pigments. The spectra also show that the fundamental band gap of Zn_2TiO_4 lies near 3.60 eV(340nm).

As shown in Table 3 the visible and infra-red reflectance values of the 900°C pigments, except in the case of the E-Series pigments, are higher than those of the 1200°C pigments; the extinction coefficients, however, show conclusively that the 900°C pigments have higher reflectance than 1200°C pigments. It should be noted that the effect of different coating weights is accounted for in calculating the extinction coefficients.

The K_{350} values (see Table 3) exhibit a definite minimum in the 1.5/1.0 - 2.0/1.0 range of the Zn/Ti ratio for both the 900°C and 1200°C pigments. E_g values also follow the same trend. E_g values are associated with Zn_2TiO_4; E_g values, with the impurity absorber. This series clearly establishes the fact that pigments whose Zn/Ti ratio is in this range possess the best reflectance values.

Comparing the spectra of the various MOX pigments with one another indicates their relative reflectance properties, but comparing each of them directly with the spectral reflectance curves for rutile titania, (r-TiO_2), anatase titania (a-TiO_2) and zinc oxide (ZnO) provides us with considerable insight. In the spectra of MOX-C(9) the fundamental absorption matches that of r-TiO_2 very closely both in slope and wavelength; that of MOX-C(12) has the same slope as r-TiO_2 but occurs at a longer wavelength. This suggests that the impurity absorption may be due to a metatitanate or other Zn-Ti-O complex. Both MOX-D(9) and MOX-D(12) have absorption bands which closely match that of r-TiO_2. MOX-E(9) and MOX-E(12) spectra contain no evidence of r-TiO_2 but do indicate the presence of ZnO; in the MOX-E(12) pigment, however, the amount of ZnO is very small.

Table 3

MOX Pigment Stoichiometry Series Results

Pigment	Reflectance Values			Coating Weight	Extinction Values[1]			Band Edge Properties[2]			
	R_{350}	R_{450}	R_{i-r}	(gms)	K_{350}	K_{450}	K_{i-r}	R_g	λ_g	E_g	E_{g_o}
MOX-C(9)	18	87	91.5	.0297	42.19	36.18	111.2	53	404	3.07	-
MOX-C(12)	17	80	84	.0266	49.25	30.13	81.06	49	407	3.07	
MOX-D(9)	12	89.5	91.2	.0291	56.99	42.52	110.6	50.5	406	3.05	
MOX-D(12)	19	89.5	89	.0705	17.01	13.56	39.27	42.7	407	3.04	
MOX-E(9)	49	83.5	85	.0515	4.88	17.81	43.71	69.5	399	3.10	3.57
MOX-E(12)	64	87	90.5	.1248	0.00	8.61	24.43	80.5	399	3.10	3.62
MOX-F(9)	49	89	89	.0665	3.78	41.54	41.53	69.5	383	3.23	3.65
MOX-F(12)	50	84	87	.0690	3.35	13.57	35.87	70.5	387	3.20	3.57
MOX-G(9)	19.5	87	92	.1071	10.95	10.03	32.26	54.5	386	3.21	
MOX-G(12)	24	82	78	.1388	6.95	6.22	12.40	55.5	393	3.15	
LH-106(12)	63	83	88	.0403	0.00	22.29	64.72				3.63

1.) See Appendix I for explanation of derivations of values.

2.) See Appendix II for explanation of derivations of values.

MOX-F(9) and MOX-F(12) pigments also contain a slight amount of ZnO. The certainty in identifying the impurity improves when, as in the case of the MOX-G pigments, the "knee" has the classic ZnO shape: the band slope matches that of ZnO, and the spectral locations of the slope changes are characteristic of ZnO. In some cases E_g is close to that of ZnO (3.297 eV). Both the spectral and K_{350} values for the MOX-G pigments indicate that the 1200°C pigment, MOX-G(12), contains less ZnO than the 900°C pigment, MOX-G(9). The same observation may also be made in the E and F series. The explanation of these observations is not clear; the fact that ZnO is formed in preference to TiO_2, however, adds further evidence for the argument that close control of stoichiometry is necessary.

This experiment strongly suggests the need to maintain the Zn/Ti ratio at or slightly below 2.0:1.0 to achieve maximum reflectance. It also suggests that, on the basis of initial reflectance, the 900°C pigments are best. Most importantly, the experiment demonstrates that close stoichiometry control is necessary in the preparation of Zn_2TiO_4 pigments from oxalate precursors.

The reflectance spectra confirm and extend the results of X-ray analyses regarding formation of TiO_2. It is clear that TiO_2 is not formed when Zn/Ti ratios are 1.5:1.0 or greater, even though Zn_2TiO_4 is formed and the titanium excess should obviously be observable as TiO_2. At the temperatures involved here only the rutile form of TiO_2 would be expected. The TiO_2 in many of the MOX materials is definitely of the rutile form, consistent with the observations that only the rutile form is found in such materials when prepared at temperatures exceeding 700°C.

The most significant finding, therefore, is that, both optically and via X-ray analysis, no TiO_2 is evident in pigments with Zn/Ti ratios of 1.5:1.0 or greater. The MOX-A pigments (with a Zn:Ti ratio of 1.49:1.0), equivalent to the MOX-E pigments of this test, exhibited excellent optical properties (but poor stability) - just as the MOX-E pigments exhibit good properties.

2.3.5 Summary

The most significant result of these experiments is the conclusion from X-ray data that relatively pure, single phase Zn_2TiO_4 is produced over a wide stoichiometry range of Zn/Ti mole ratio, viz., from 1.5:1.0 to 2.0:1.0. This is difficult to understand for the 1.5:1 ratio since a definite excess of TiO_2 (0.33 mols) should exist. However, the optical spectra also contain no evidence of free TiO_2 in MOX-E material. This is consistent with and confirms identical observations made in the case of MOX-A materials. Reflectance spectra suggest a pure Zn_2TiO_4 for MOX-E(12) and a somewhat less pure material for MOX-E(9). Gravimetric data also show that the weight loss encountered at 900°C (0.20%) is much too small to indicate a loss of material such as TiO_2. Furthermore, the vapor pressure of TiO_2 at these temperatures is far too low for any volatilization to occur, which might otherwise explain this absence.

It is unlikely that the composition of the pigments differ significantly from those experimentally designed, i.e., a composition in which the Zn/Ti mole ratio in the "oxalate" precursor mixture is 1.5:1.0, for example, should maintain through a 1200°C calcination. Chemical analyses may be necessary to eliminate (or confirm) this possibility as the reason for the anomalous results.

A distinct possibility in explaining the absence of TiO_2 is that the MOX-E material may have a composition such as:

$$3Zn_2TiO_4 + Zn_2Ti_3O_8 + ZnO$$

Zinc sesqui-titanate ($Zn_2Ti_3O_8$) has the same crystal structure as Zn_2TiO_4, with a slightly smaller lattice parameter (8.395Å vs 8.456Å). Since these compounds have such similar lattices, distinguishing them by X-ray analysis was difficult particularly in fine powders where line broadening occurs. Careful analyses of the back-reflection patterns of the above, except for a positive indication of ZnO, indicate the presence of $Zn_2Ti_3O_8$. The finding of the sesquititanate without finding ZnO, however, requires further analyses and studies to define the nature of the oxalate-titanate chemistry.

Our previous assumption that an excess ZnO composition of 2.05 Zn:1.00 Ti is necessary for obtaining TiO_2-free Zn_2TiO_4 obviously does not apply to the oxalate precursor methods. The present work shows that Zn-deficient oxalate precursors with a Zn/Ti ratio of 1.5:1.0, when calcined, will produce a material exhibiting excellent reflectance, similar to that for a pure Zn_2TiO_4. MOX-A materials however, demonstrated poor stability to ultraviolet irradiation in vacuum (Ref. 2). The results of MOX-A tests would, therefore, suggest that stoichiometries with a Zn/Ti ratio as close as possible to (but less than) 2.0:1.0 would be ideal, because they would result in pigments with no ZnO excess, no TiO_2 excess and a minimum of less stable titanate species. The question of environmental stability, however, still remains to be answered.

2.4 Ball-Milling Experiments

To test the effect of ball-milling their oxalate precursors (i.e., prior to calcination) on the particle size and optical properties of pigments, samples of a COP precursor material and of a "MOX" material were subjected to a controlled ball-milling experiment. The ball-milling was accomplished using a ball-to-charge ratio of 1:1 and a ball-milling time of 16 hrs. After ball-milling the samples and the control (i.e., unball-milled) materials, the precursors were pre-calcined at 600°C/2hr and then calcined at 1200°C/2hr.;

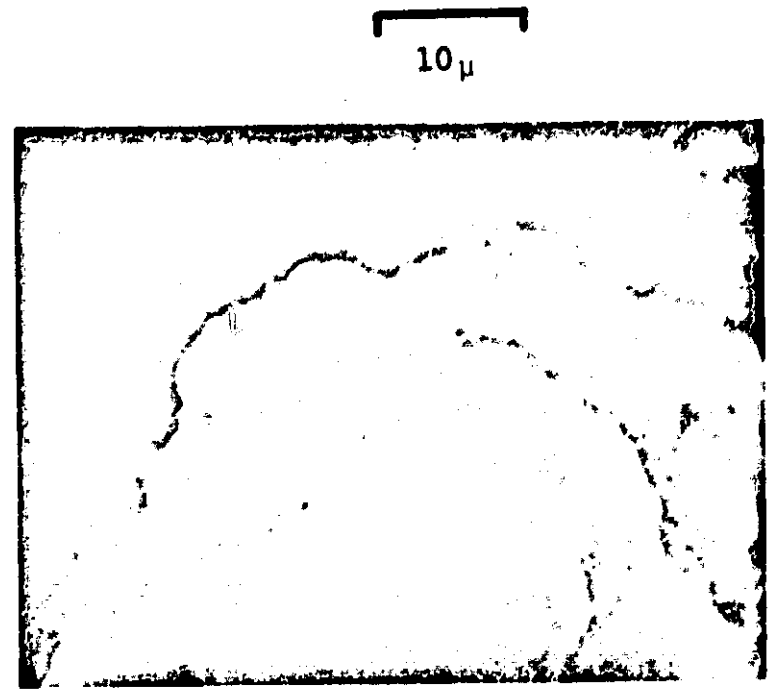
Sample	600°C/2hr	1200°C/2hr
LH-105	X	X
LH-105 BM*	X	X
MOX-A	X	X
MOX-A BM*	X	X

*Ball milled 16 hrs at a ball-to-charge ratio of 1:1.

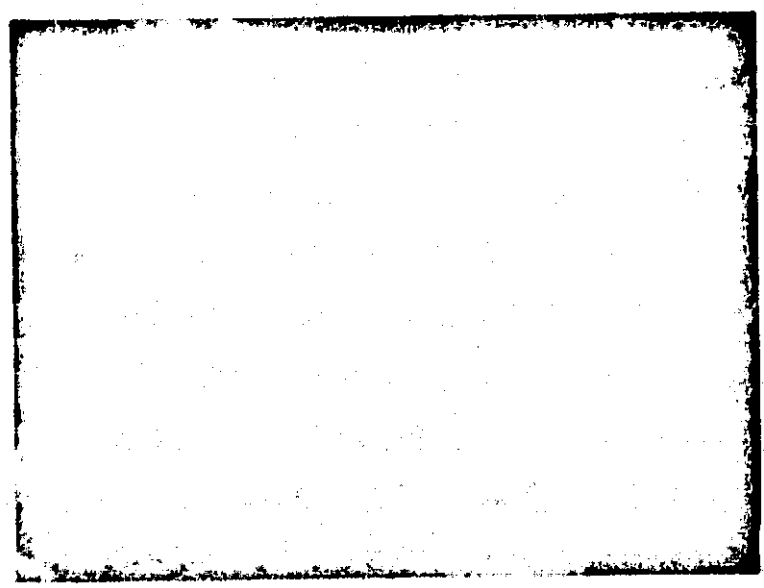
2.4.1 SEM Investigations

Examination of the SEM photomicrographs of these materials showed that the particle size of the ball-milled, uncalcined powders was somewhat finer than the non-ball-milled powders and showed fewer agglomerates (Figures 10 and 11). For the pigments prepared at 600°C, these relationships were still evident, as Figures 12 and 13 show.

For the 1200°C calcined materials, such differences were not as evident. In the ball milled samples, LH-105(6-12)BM and MOX-A(6-12)BM, the larger particles were about the same size as those in the non-ball milled, i.e., about 3-5μ (Figure 14 and 15. However, there was definite evidence of finer particles and of less necking for the BM samples, as compared to the non-ball milled.



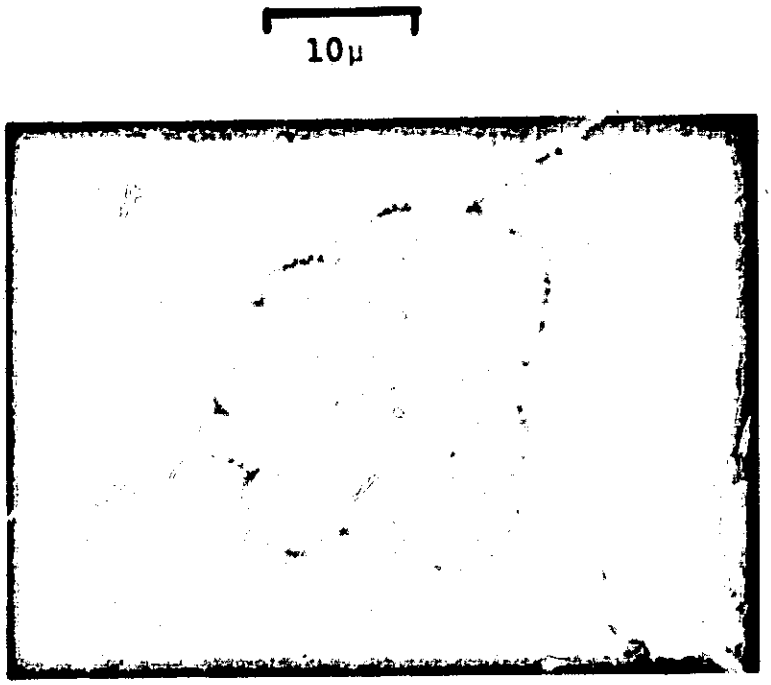
520 MOX-A 3000X



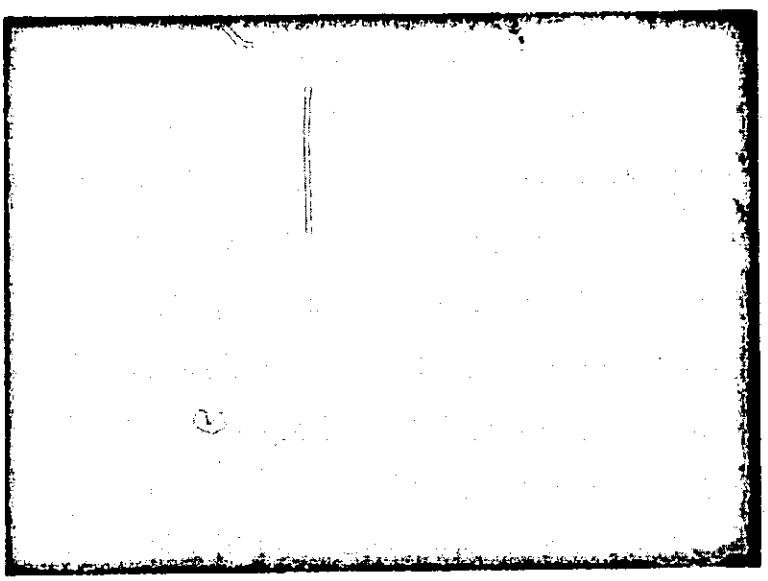
521 MOX-A(BM) 3000X

Figure 10 SEM Views of MOX-A and MOX-A Ball Milled

ORIGINAL PAGE IS
OF POOR QUALITY



522 LH-105 3000X



530 LH-105(BM) 3000X

ORIGINAL PAGE IS
OF POOR QUALITY

Figure 11. SEM Views of LH-105 and LH-105 Ball Milled

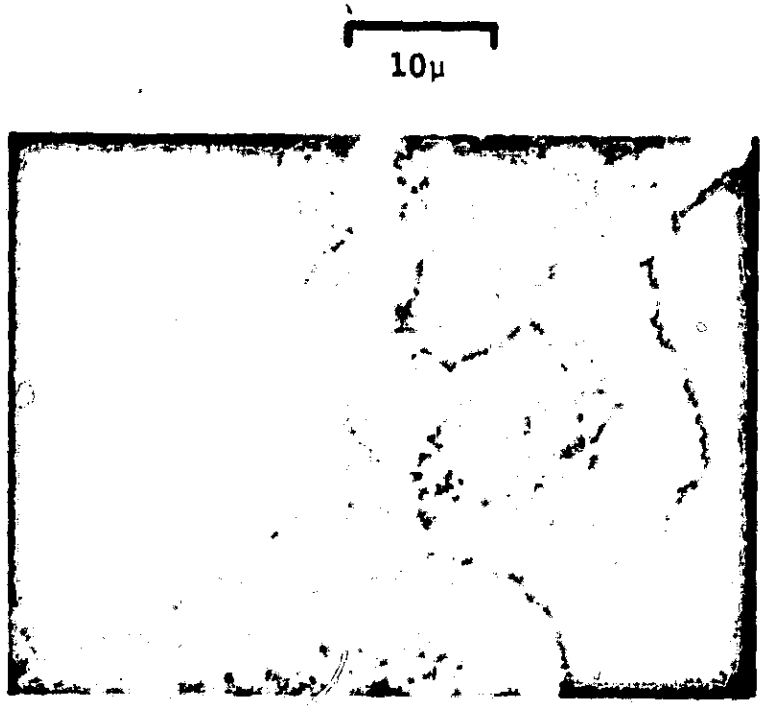
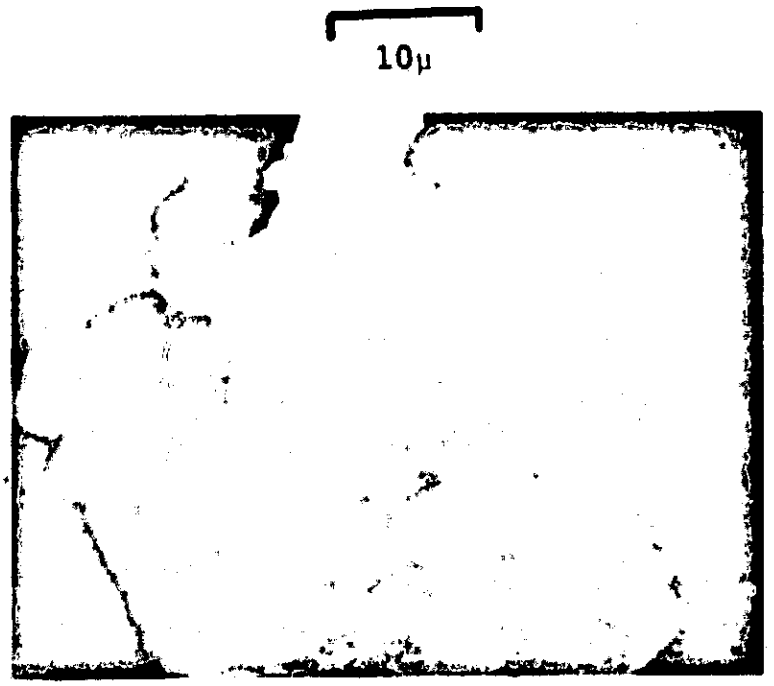


Figure 12. SEM Views of MOX-A and MOX-A Ball Milled, Calcined at 600°C/2 Hrs.

ORIGINAL PAGE IS
OF POOR QUALITY



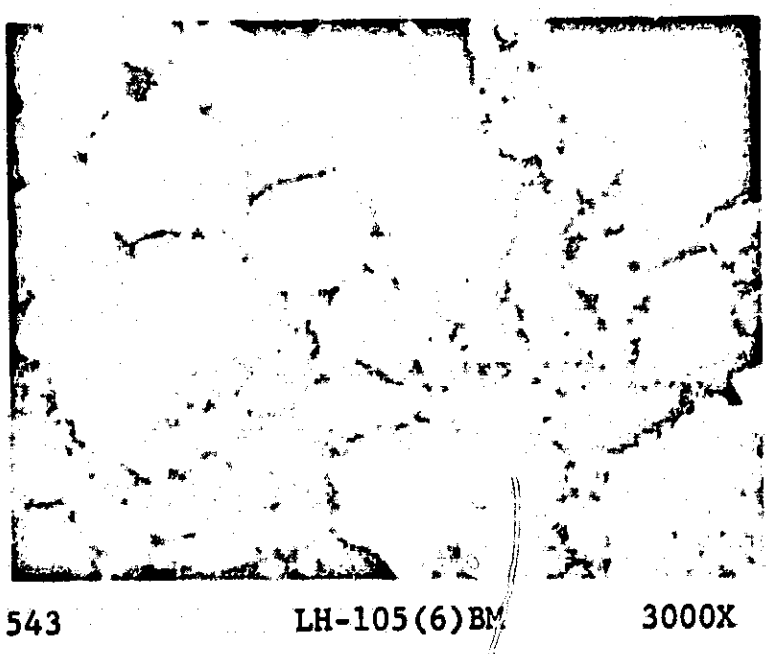
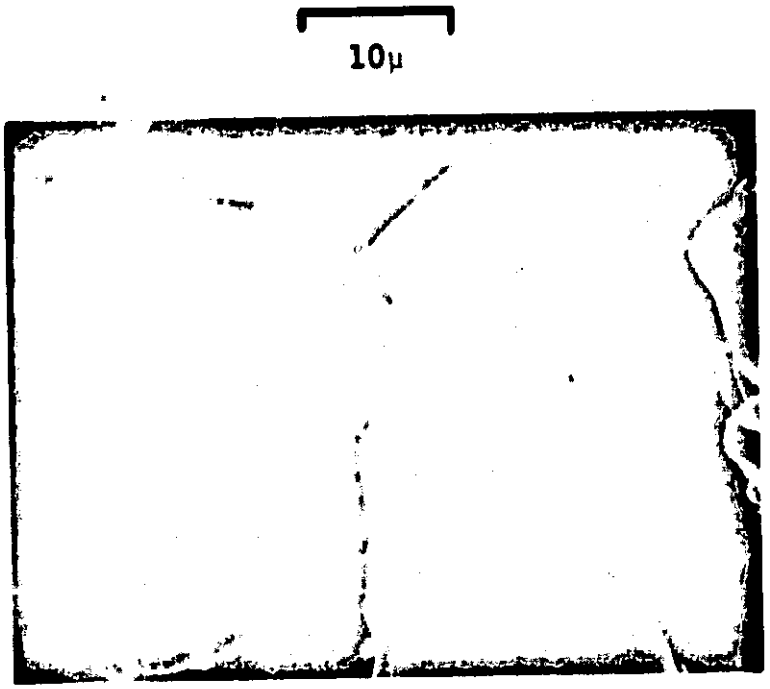


Figure 13. SEM Views of LH-105 and LH-105 Ball Milled, Calcined at 600°C/2 Hrs.

ORIGINAL PAGE IS
OF POOR QUALITY



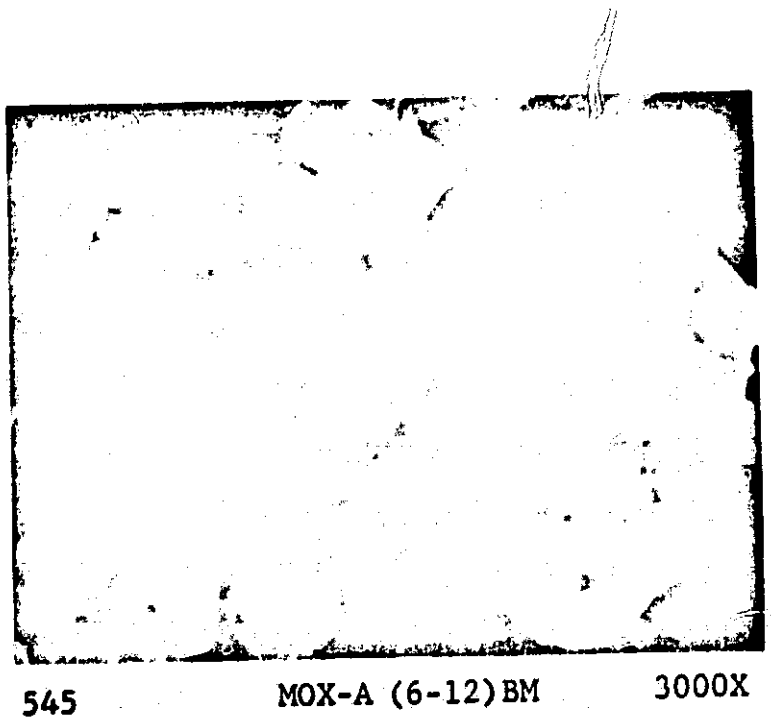


Figure 14. SEM Views of MOX-A and MOX-A Ball Milled, Calcined at 1200°C/2 Hrs.

ORIGINAL PAGE IS
OF POOR QUALITY



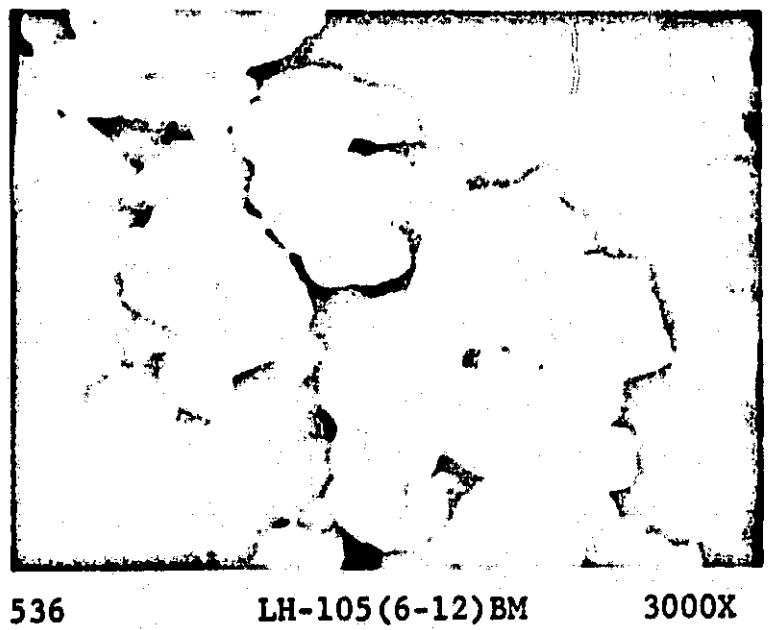


Figure 15. SEM Views of LH-105 and LH-105 Ball Milled, Calcined at 1200°C/2 Hrs.

ORIGINAL PAGE IS
OF POOR QUALITY

2.4.2 Optical Investigations

The pigments described above were sprayed onto IRIF coupons as powders. Diffuse reflectance spectra were then recorded in the spectral range 325-2600nm. Figs. 16 and 17 show these spectra in the 325-500nm range; the spectra of the powders in the 500-2600nm region is essentially flat.

Table 4 lists the pertinent data, presented similarly to those in Table 3. Because of the very high reflectance values at 350nm, the reference value of reflectance at 350nm, i.e., R_{350}, was taken as 70%. The other extinction values refer to R_∞ = 95%. The reflectance levels in both the COP and MOX pigments are higher for ball-milled pigments than for control pigments. The visible and i-r extinction values, particularly in LH-105, indicate the converse. The decrease in K_{450} with ball-milling implies that ball-milling adversely affects visible reflectance. The higher reflectance values of the ball-milled pigments, however, may result from the greater apparent thickness of the coating, which in turn may be due to better packing in ball-milled pigments. The slope of the absorption band, especially in the MOX-A pigment, has been altered by ball-milling, indicating that the effective particle size distribution has been extended.

An improvement in reflectance properties does occur as a result of ball-milling. The effect of ball-milling on optical stability remains to be determined, but previous tests showed no damage attributable to ball-milling.

2.5 Evaluation of SRI Treated Pigments-Sprayability

Test samples of Zn_2TiO_4 with various surface treatments were forwarded by Dr. K.M. Sancier of Stanford Research Institute (SRI) to IITRI for a determination of their sprayability as

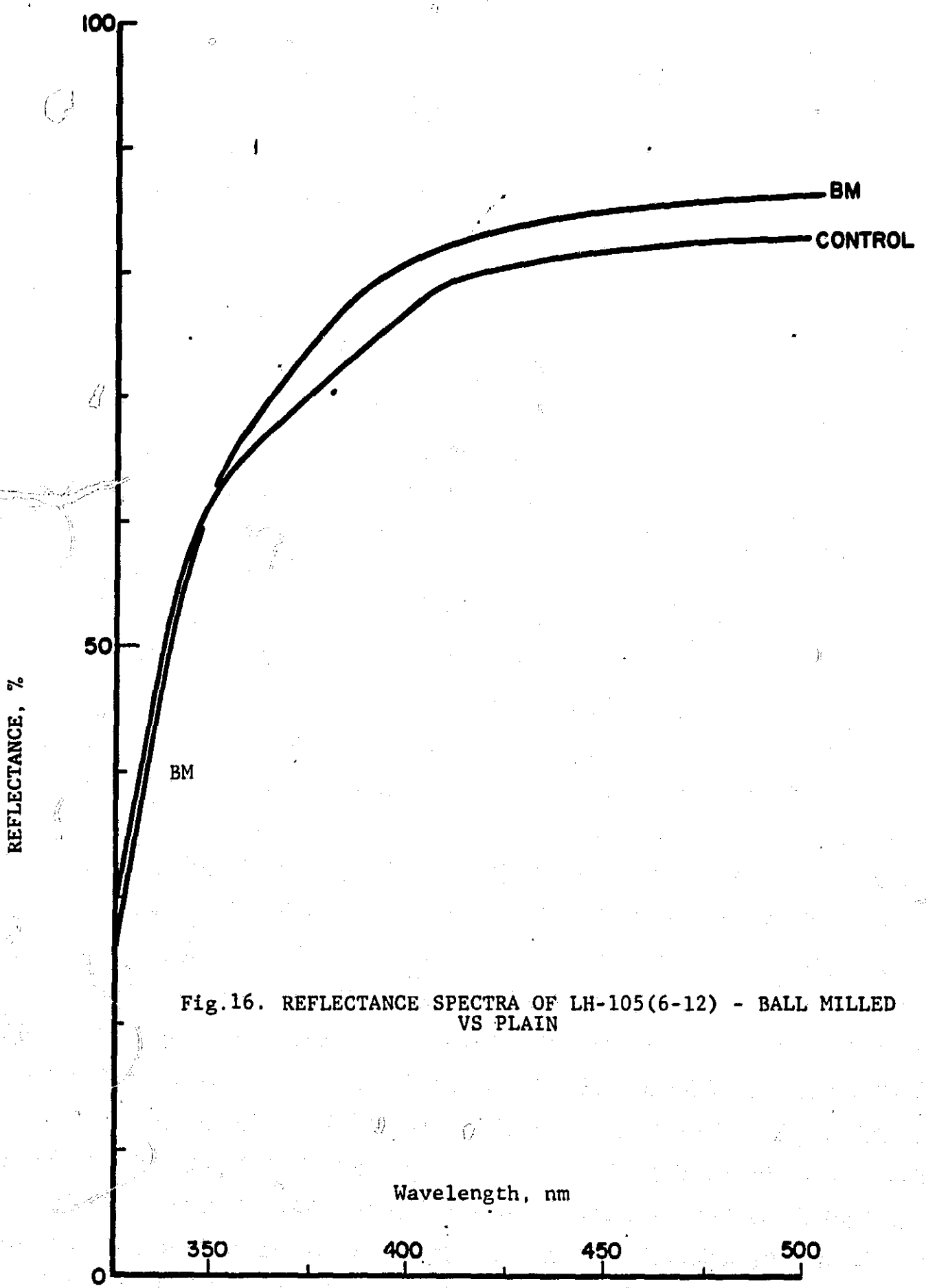


Fig.16. REFLECTANCE SPECTRA OF LH-105(6-12) - BALL MILLED VS PLAIN

C6233-48

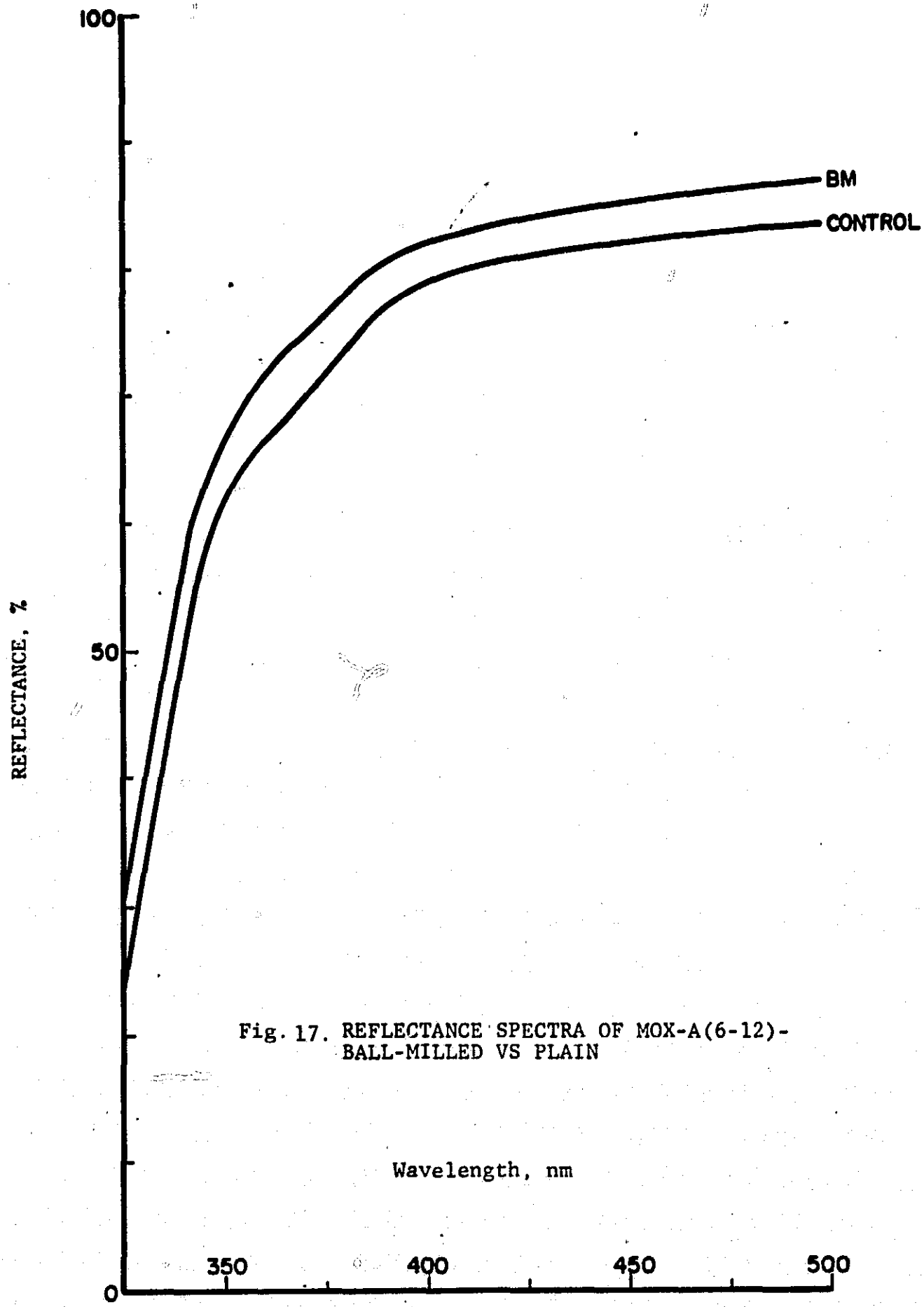


Fig. 17. REFLECTANCE SPECTRA OF MOX-A(6-12)-BALL-MILLED VS PLAIN

C6233-48

Table 4

Ball-Milled Zn_2TiO_4 Pigment Data

Pigment	Reflectance Values			Coating Wt, gms.	Extinction Values			Band Edge Properties		
	R_{350}	R_{450}	R_{i-r}		K_{350}*	K_{450}	K_{i-r}	R_{go}	λ_{go}	E_{go}
LH-105(6-12)	62.3	81.8	85.5	.0454	2.567	43.48	50.73	55.5	34.19	3.62
LH-105(6-12)BM	62.7	84.9	89.0	.0813	1.355	27.57	33.98	55.2.	34.25	3.61
MOX-A(6-12)	62.3	81.5	86.0	.0710	1.642	27.48	33.20	53.4	34.25	3.61
MOX-A(6-12)BM	66.5	84.9	88.5	.0836	0.613	26.81	32.09	58.1	34.06	3.63

*The reference value of reflectance at 350nm in this series is 70%; in table 3, it is 63%.

powders and as OI650G paints. The Zn_2TiO_4 in this case was taken from a batch which earlier was found to have been slightly contaminated. Table 5 summarizes our observations.

Table 5

Observations of Sprayability

SRI Sample No.	Treatment	Powder*	Paint		Remarks
			Before Bake	After Bake	
1	0.01M Ce^{+3}/Ce^{+4}	White	White	Brown	Both Spray OK
2	0.001M Ce^{+3}/Ce^{+4}	"	"	Light Brown	" "
3	0.1M $HClO_4$	"	"	Slight Discoloration	
4	1N HF	"	"	Slightly off-white.	Lumps on spraying, does not harden in OI650G

*Powder films were sprayed from a H_2O slurry.
**OI650G films were air-cured overnight and baked 325°F/16hr.

In general these pigments are not compatible with the OI650G resin. The coloration of the films may result either from an interaction between the treatment ion and one or more of the solvents in the OI650G thinner or as a result of a surface contaminant reaction with the silicone. The primary purpose of these tests, however, was to determine whether Zn_2TiO_4 treated in various manners as above could be sprayed as powders and as OI650G paints. While the HF treated pigments show considerable reactivity, all the pigments tested can be sprayed both as powders and as paints.

Table 6

Behavior of SRI Powders

Pigment	Treatment	Powder	Paint	Paint Baked 325°F
237-65-1	Ce^{3}/Ce^{+4}	Bright off-white	Med. off-white	Brown
237-65-2	$Fe(CN)_6$	Med. off-white	Cream off-white	Grayed off-white
237-65-3	$Ir\ Cl_6\ 10^{-2}M$	Sl. Gray off-wyite	Sl. Gray off-white	Yellowed off-white

Powders, Unbaked		Paint, Unbaked	Paints Baked ea. 325°F
Brightest	237-65-4	237-65-1	237-65-2
	237-65-1	237-65-2	237-65-4
	237-65-2	237-65-4	237-65-3
Darkest	237-65-3	237-65-3	237-65-1

By far the greatest darkening on baking was the Ce doped material (as in a previous sample). The least darkening on baking was the $Fe(CN)_6$ doped material.

A repeat test was made of the treated pigments in the same manner as above; the results, as Table 6 shows, were similar.

In an effort to determine whether the coloration upon heating of the paint is caused by one of the solvents in the OI-650G thinner, the following mixes were made with a cerium treated Zn_2TiO_4 pigment. (A total of only 5 grams was available).

1. A dry mull of the pigment with powdered solid OI-650 resin. No solvents were used.
2. A wet mull with the pigment in OI-650G resin at a 70% concentration in toluene.
3. A wet mull of the pigment with OI-650G resin in butyl acetate.
4. A small jar mill grind of the pigment in RTV-602 thinned slightly with toluene to permit grinding.

Each of the above was applied to two sets of aluminum coupons which had been thoroughly cleaned and, in the case of the RTV-602, primed with SS4044, but no catalyst for the RTV602 was used. One set of coupons was allowed to air dry 18 hrs; the other set was baked, 18 hours at 325°F.

In all cases the air dried coupons showed no discoloration in 18 hours; the baked coupons discolored severely. The worst discoloration was with the OI-650G in toluene. The butyl acetate thinned resin was less discolored.

The intense discoloration on baking even with no solvent present disposes of the theory that the solvent is to blame for the darkening of the cerium activated pigment. It is important to note that the unbaked coupon of the paint made from an RTV vehicle did not discolor at room temperature but

did not dry (since uncatalyzed). The baked specimen dried perfectly but did discolor. These results tend to indicate that surface contamination of the pigment was principally responsible for the discoloration. More recent tests with SRI-heated pigments (which were not surface contaminated) revealed no discoloration in OI650G paints after heat-curing, confirming the above conclusion. In all cases the SRI treated pigments are sprayable both as pigments and as OI650G paints.

3. CHARACTERIZATION OF OXALATE PRECURSORS

3.1 Background

The underlying basis for the production of zinc orthotitanate, Zn_2TiO_4, from oxalate precursors resides in the instability of the "oxalates" when heated and in the eventual reaction of the "oxalates" or their reduction products to form Zn_2TiO_4. The chemistry of the reactions, however, has not been well understood. In previous studies of Zn_2TiO_4 pigments, it had been established that an excess of ZnO in the Zn_2TiO_4 product is necessary. The presumptions were that a ZnO excess could be removed by appropriate chemical treatment, whereas a TiO_2 excess could not, and that a ZnO excess would not promote Zn_2TiO_4 degradation, whereas TiO_2 would.

The data on MOX-A pigments have raised some very important questions regarding the validity of the ZnO excess requirement. This series of pigments was prepared (in a laboratory error) at a Zn/Ti mole ratio of 1.49 rather than 2.05 as is ordinarily done. While some of the Zn_2TiO_4 pigments prepared from the MOX-A precursors showed evidence of a TiO_2 excess in their reflectance spectra, there were several with excellent ultraviolet reflectance spectra, indicating no substantial excess of either TiO_2 or ZnO. It was observed that the MOX-A pigments calcined at higher temperatures evidenced no TiO_2 excesses. Other observations were made and conclusions reached regarding MOX-A pigments (Ref. 2), which have prompted the analytical studies described here.

3.2 Process Chemistry

In light of the questions raised in regard to the proper Zn/Ti ratio and their implications, we believe it necessary to establish conclusively the chemical nature of the products of

the precipitation process, and the chemical reactions involved in their high temperature conversion to oxides. Although a specific test was not made to assure that the Zn and Ti compounds produced in the coprecipitation process are identical to those produced when precipitated separately, there is much indirect evidence, including SEM photomicrographs to suggest that they are.

The precipitation and subsequent calcination processes have been described by the reaction(s):

$$\left.\begin{array}{l} 2ZnCl_2 + 2H_2C_2O_4 \longrightarrow 2ZnOx \\ TiCl_4 + H_2C_2O_4 \longrightarrow \text{"TiOx"} \end{array}\right\} \xrightarrow{\Delta} Zn_2TiO_4$$

In the coprecipitation (COP) process, the chlorides of Zn and Ti in the mole ratio of 2.05 Zn/Ti are added simultaneously to an aqueous oxalic acid solution. The resultant precipitate presumably also contains a 2.05 Zn/Ti mole ratio. In the "MOX" process the precipitates obtained from chloride addition are obtained individually; the resulting precipitates, i.e. "ZnOx" and "TiOx", are mixed to obtain a 2.05 Zn/Ti mole ratio, then ball-milled to ensure adequate mixing. In both cases the resulting "co-precipitate" is calcined to obtain Zn_2TiO_4 pigment.

3.3 Oxalate Molecular Weight Determinations

3.3.1 Zinc Oxalate

An obvious requirement in achieving a 2.05 or any other specific Zn/Ti mole ratio is that the molecular weights of the ZnOx and "TiOx" compounds must be known. Because of the uncertainty in the actual effect of stoichiometry inherent in the MOX-A irradiation test results (IRIF Test No. I-71), we undertook a complete review of the bases for process chemical calculations. Purposely, we have avoided up to this point any

reference to the actual chemical nature of "ZnOx" and of "TiOx" (the solid reaction products of $ZnCl_2$ and of $TiCl_4$, respectively, with $H_2C_2O_4$).

Samples of ZnOx and of "TiOx" were individually subjected to SEM and x-ray analyses, and were calcined at various temperatures. From mass loss, SEM and x-ray data and analyses of reflectance spectra of the precursors and their products, we have shown that "ZnOx" is $ZnC_2O_4.2H_2O$. The mass loss data, for example, show that ZnOx is almost completely converted to ZnO at 500°C, and that the ultimate weight loss is 57.4 weight percent (w/o) of the original weight. This implies a conversion of (1.0-0.574)x100%, or 42.6 w/o. The formula weight of $ZnC_2O_4.2H_2O$ is 189.43; and of ZnO, 81.38. The ratio of their molecular weights (ZnO/ZnOx) for 100 w/o conversion, is 0.4296. The identification of "ZnOx" as $ZnC_2O_4.2H_2O$ is consistent with experimental evidence and with formulae given in the literature (e.g., ref. 3). We are thus quite certain of this assignment.

3.3.2 "TiOx" Molecular Weight

The chemical formula of "TiOx" and thus its true molecular weight can not be obtained as simply. It depends upon temperature-induced mass-loss data corroborated by other evidence. Literature references are sketchy at best and not directly applicable. Tables 7 and 8 present the available data on static and TGA mass loss of "TiOx"; Fig. 18 shows fractional mass vs time for the TGA test. The reaction, at sufficiently high temperatures leads to the production of anatase titanium dioxide; thus,

$$\text{"TiOx"} \xrightarrow{\Delta} TiO_2$$

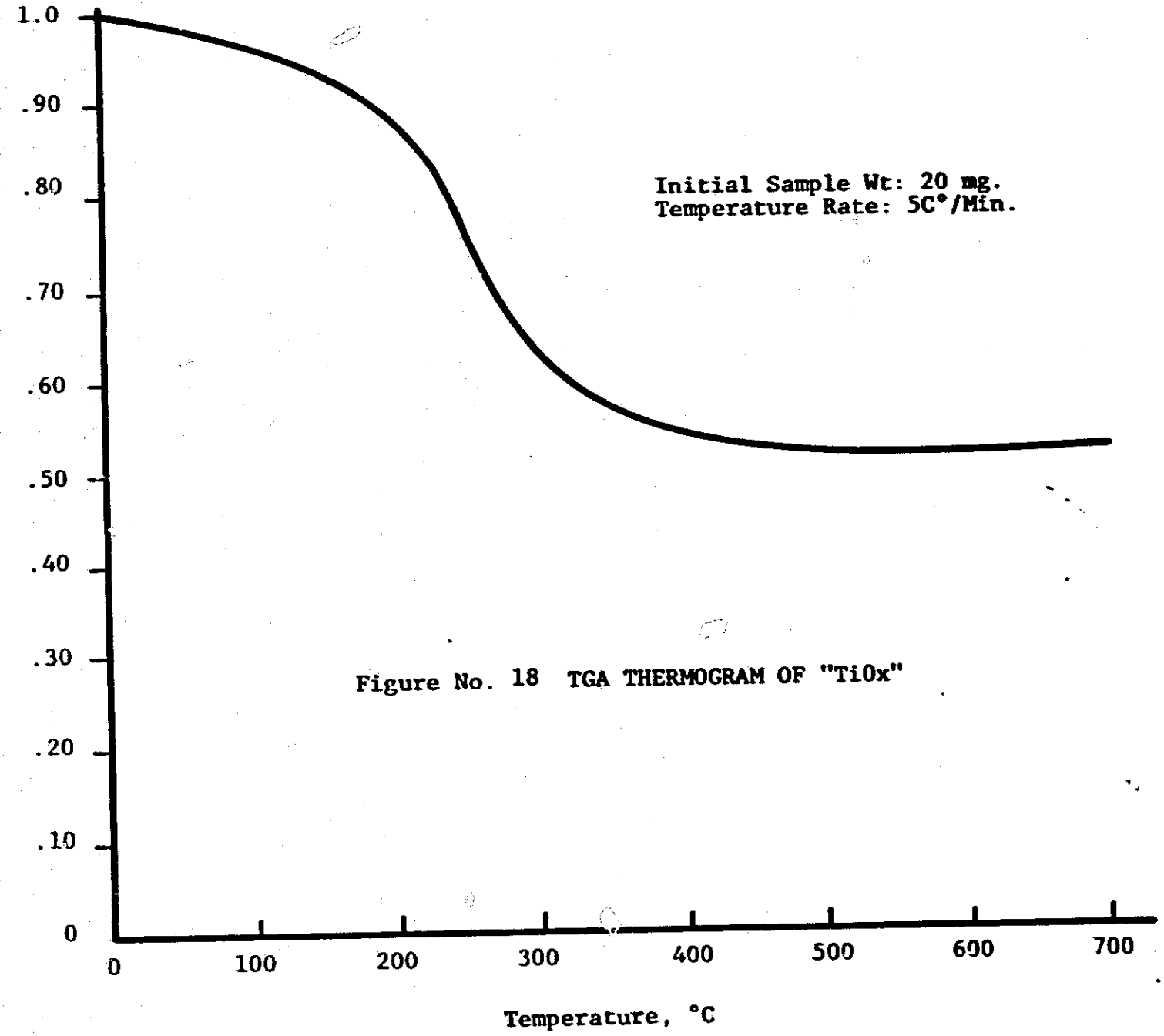


Figure No. 18 TGA THERMOGRAM OF "TiOx"

C6233-48

Table 7

Mass Loss Data
Stati. Calcination Data

Temp (°C)	Time (Hr)	Weight Loss, %	FML* Conversion	Yield**
150	1	6.96	.1491	.0242
	4	8.07	.1729	.0512
	48	8.46	.1813	.0606
230	.083	17.44	.3737	.2791
	1	39.92	.8555	.8261
	4	44.34	.9503	.9336
340	.083	43.73	.937	.9188
	1	44.43	.9522	.9358
	4	44.89	.9621	.9470
500	1	45.56	.9764	.9633
	4	45.52	.9756	.9623
700	1	46.66	1.0000	.9901
	4	46.37	.9938	.9830

*FML - Fractional Mass Loss (=% mass loss/maximum % mass loss), relates to overall reaction completion.

**Yield - Moles fraction of TiO_2 formed/mole of "TiOx".

Table 8
TGA Data

Temp (°C)	FMR*	FML*	Yield**
25	1.000	0.000	.0000
75	.982	.0373	.0000
100	.969	.0642	.0000
150	.937	.0130	.0081
200	.894	.2195	.11271
250	.785	.4451	.3779
300	.625	.7764	.7672
350	.568	.8944	.9059
400	.553	.9255	.9424
450	.522	.9896	1.000
500	.517	1.000	1.000
600	.517	1.000	1.000
700	.517	1.000	1.000

*FMR = Fraction of original mass remaining;
FML = Wt. loss/max. wt. loss (=1-.517)

**Yield = mole fraction of TiO_2 formed/mole of "TiOx"

The highest yield obtained (in terms of mass loss) was 46.66%, or 53.34% conversion of "TiOx" to TiO_2. The molecular weight of TiO_2 is 79.90. Therefore, the inferred molecular weight of "TiOx" is 79.90/0.5334 = 149.79 (the last decimal place is not significant). TGA data (see Table 8) confirm this calculation. This value is in fact the one used in preparing MOX pigments. The only literature available (e.g., ref. 3) lists $Ti_2(C_2O_4)_3.10H_2O$ with a molecular weight of 540.01. Clearly this is not the product obtained in the precipitation process.

The mass loss data of tables 7 and 8 are shown in fig. 19, where the log of the conversion (of the "TiOx" precursor to TiO_2) is plotted vs 1/T(°k). This method of presenting the mass loss data will be examined subsequently in greater detail. The conversion is determined as the ratio of the product mass at any temperature and time conditions to the ultimate (or maximum) mass. In the extant case, calcining beyond 500°C produces no additional mass loss, and the ultimate fractional mass is 0.5334 from static data and 0.517 from TGA data. The difference (about 1-1/2%) may be due to batch-to-batch variations or slightly different pre-treatment conditions. The extrapolation of the conversion data in the low temperature region in fig. 19 to 0.0 (100% completion) intersects at a temperature of 235°C for the static data and at 300°C for the TGA data. The difference arises because static data represent equilibrium conditions, TGA data very likely do not, although they exhibit consistency.

The true minimum molecular weight of "TiOx" can be inferred from the static data by correcting its molecular weight by the weight loss below 235°C, thus, by the factor (1 - 0.0846) = 0.9154. The minimum molecular weight of the true "TiOx" is then 149.79•0.9154 = 137.12. Hence, for clarification, we have

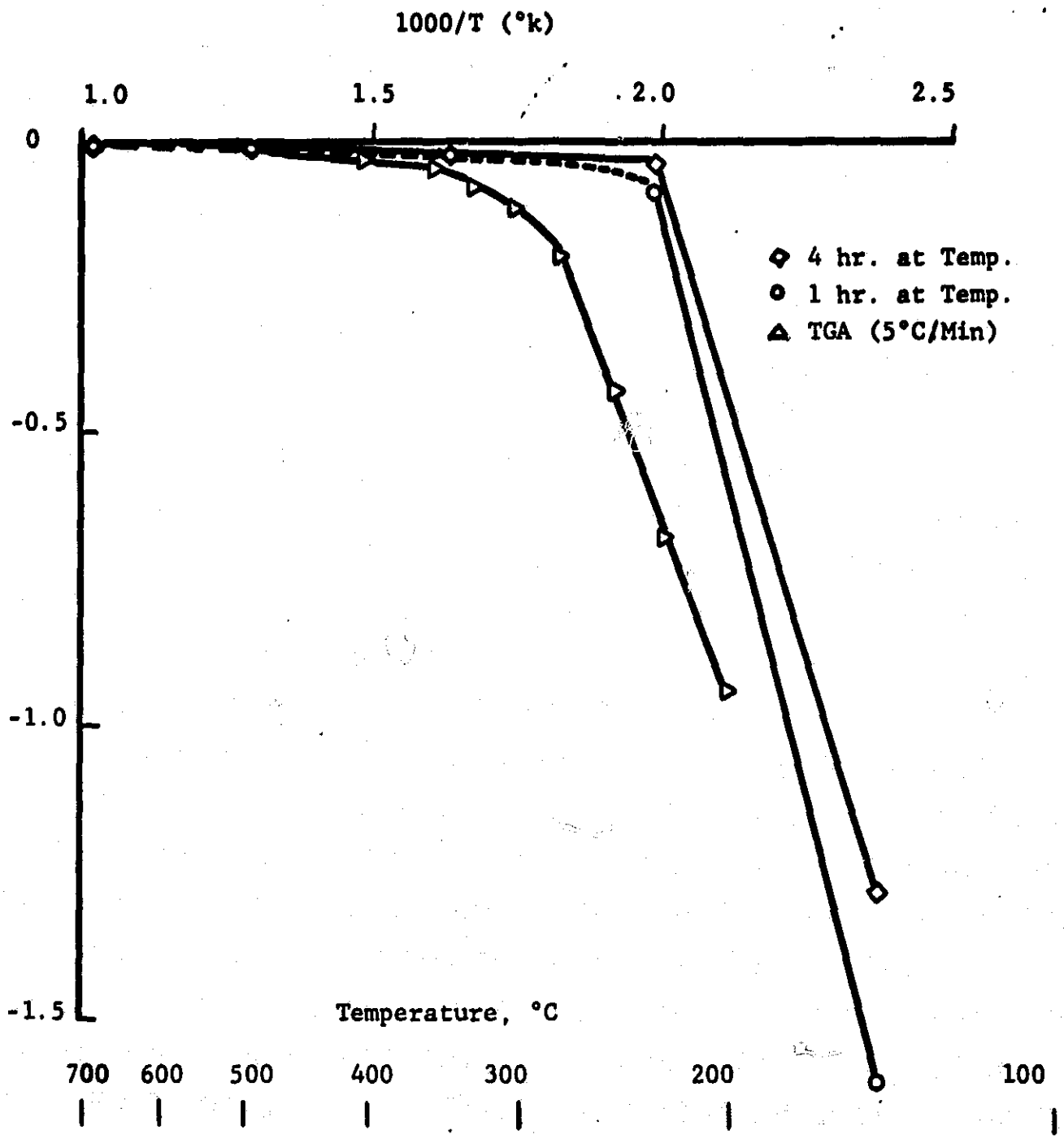


Figure No. 19 "TiOx" CONVERSION VS RECIPROCAL TEMPERATURE

"wet" TiOx, i.e., $TiOx \cdot nH_2O$, with an actual (effective) molecular weight of 149.79 and "dry" TiOx with a minimum molecular weight of 137.12. In practice only the "wet" TiOx is used, and the term "TiOx", unless otherwise noted will refer to $TiOx \cdot nH_2O$.

The molecular weight of 149.79 is easily within an accuracy of ± 5%; thus it clearly rules out any possibility that TiOx is a double oxalate, since $Ti(C_2O_4)_2$ has a molecular weight of 223.94. The radical TiC_2O_4 ++, however, has a molecular weight of 135.92. This suggests that "dry" "TiOx" may be $H_2TiC_2O_4$ and that "wet" TiOx is $H_2TiC_2O_4 . 0.7\ H_2O$. Chemical analyses of "wet" "TiOx" have shown that the carbon content is in the range 9.3 - 9.7 w/o and that its hydrogen content is approximately 2.5 w/o. The carbon content would argue strongly against "TiOx" being an oxalate since the two oxalate carbons in "TiOx" would contribute in excess of 16 w/o. A more likely formula is $Ti(OH)_2CO_3$ with a molecular weight of 141.94; with a half mole of water of hydration, the mol. wt. becomes 150.95 (very close to the value of 149.79, and within experimental error). With this formula the theoretical values of carbon and hydrogen content also lie well within experimental error for the physical test values. The justification for this selection follows from the fact that the data from Fig. 17 only set an upper limit to water content; the shape of the curve at values of higher mass loss may, and very probably do, reflect some oxalate decomposition rather than, as we have assumed, only water evolution. The opposite, however, is not true. Further, the reaction of $TiCl_4$ with water is known (Ref. 4) to produce a stable tetravalent hydroxide. In an aqueous solution of oxalic acid, there would be a competition between the H_2O and the oxalic acid for reaction with the $TiCl_4$. We assume that the following reaction scheme prevails in the precipitation process:

$$TiCl_4 + 4H_2O \rightarrow Ti(OH)_4 + 4HCl + 2H_2\uparrow$$

$$Ti(OH)_4 + 1/2\ H_2C_2O_4 \rightarrow Ti(OH)_2CO_3 + H_2O + 1/2\ H_2\uparrow$$

From our analyses of the mass loss data, it is reasonable then to postulate that the reactions of TiOx when heated are:

$$Ti(OH)_2CO_3 \cdot 0.5H_2O \xrightarrow{\Delta} Ti(OH)_2CO_3\uparrow + 0.5\ H_2O\uparrow$$

$$Ti(OH)_2CO_3 \xrightarrow{\Delta} TiO_2 + CO_2\uparrow + H_2O\uparrow$$

3.4 "TiOx" Characterization

A further analysis of the data in Table 7 was carried out to establish the reaction kinetics of the "TiOx" calcination. The Clausius-Clapeyron equation was used to calculate the heat of reaction. The appropriate reduced static data are plotted in Fig. 16, along with those of the TGA, as the logarithm of the percentage completion of the reaction vs the inverse temperature 1/T(°K). From this plot it is quite obvious that different reactions occur as a function of temperature. In the temperature range below 230°C the heat of activation is very high (11815 cal/mole,) close to that expected from the desorption of water of hydration (9729 can/mole). The abrupt change in slope at about 1.98×10^{-3} (∿225°C) occurs also in the TGA spectrum (Fig. 17). A close comparison between these and TGA data should not necessarily be expected, since these data were obtained under essentially static conditions (by subjecting "TiOx" to specific temperatures for pre-determined times) while the TGA data reflect instantaneous, not necessarily equilibrium weight loss. Fig. 17 is based on the Arrhenius equation:

$$K = \frac{k_1}{k_2} = S \cdot \exp(-\Delta H_A/RT) \qquad (1)$$

In logarithmic form, eq. 1 becomes

$$\text{Log } K = \log S - \Delta H_A/RT \qquad (2)$$

These equations provide a powerful analytical tool, especially when the reactions involved are in, or very nearly approach, equilibrium. Eq. 2 may be re-written in the form

$$y = A - Bx, \qquad (3)$$

where $y = \log K$

$A = \log S$ (a constant)

$B = \Delta H_A/R$ (a constant)

$x = 1/T$

An endothermic reaction which exhibits a temperature dependence can be analyzed to determine ΔH_A. Note that in fig. 17 the slope of log K vs 1/T, and thus the heat of reaction, changes abruptly. This signifies that the nature of the reaction is very different at temperatures above ∿225°C. Other points to note in fig. 17 are the close similarity of the 1 hr and 4 hr static data in the low temperature region and the apparent discrepancy between static and TGA data. The slope of the TGA data is very close to those of the static data. From the displacement in static and TGA data we infer a significant time-dependence of the reactions; the TGA reaction at a constantly increasing temperature does not have sufficient time to reach completion. This is further evidenced by the fact that the displacement in the low temperature region, as expected, remains relatively constant with increasing temperature. Significantly, however, both the TGA and static data show a close correspondence above 225°C. The reason, of course, is that the heat of reaction is considerably smaller (approximately 1575 cal/mole) and the time dependence, likewise is much less. The static and TGA data are consistent in predicting a heat of reaction of about 1550 cal/mole from the conversion of "TiOx" to TiO_2. This would tend to

indicate that the oxalate precursors do not react differently as a function of temperature - at least not in terms of the reaction energy. The analysis of mass loss data via the Arrhenius and the Clausius-Clapeyron equations is developed in greater detail in Appendix III.

3.5 Conclusions

Our analyses show rather conclusively that the zinc precursor is $Zn_2C_2O_4 \cdot 2H_2O$. Less certain, however, is the formula for "TiOx" the titanium precursor. Mass loss data indicate that its molecular weight is approximately 149.8 (137.1 in the "dry" state). The formula inferred from these data is $Ti(OH)_2CO_3 \cdot 0.5H_2O$. It is certain that "TiOx" is not an oxalate. A Clausius-Clapeyron analysis shows two distinct regimes; a low temperature region (T<200°C) where the heat of reaction (~11800 cal/mole) reflects a water desorption process, and a higher temperature region (200-500°C) in which "TiOx" converts to TiO_2 with a heat of reaction of about 1575 cal/mole.

APPENDIX I

Calculation of Extinction Values

Extinction can occur either through absorption of reflection (or both). The extinction coefficients usually are defined by the Beer-Lambert Law:

$$I = I_o e^{-Kx} \qquad (I\text{-}I)$$

where

I = emergent flux intensity
I_o = incident flux intensity
K = extinction coefficient
x = thickness

The value of K, therefore, is determined from the solution of eq. I-1.:

$$K = \ln(I_o/I)/x \qquad (I\text{-}2)$$

For the calculation of K_{350}, we use the relationship, $R_{350} = 63 \cdot e^{-Kx}$, or

$$K = \ln(63/R_{350})/x \qquad (I\text{-}3)$$

Eq. I-3 is formulated on the assumption that 63% is the highest reflectance a zinc orthotitanate pigment would exhibit at 350nm; the reference material is LH-106(6-12). K, in this instance, is a measure of the impurity absorption which reduces the reflectance of the Zn_2TiO_4 at 350nm.

The extinction values, K_{450} and K_{i-r}, were calculated from a similar relationship:

$$R = R_\infty (1-\exp(-K_s x)) \qquad \text{(I-4)}$$

In this formulation K_s becomes a measure of the scattering effectiveness of the pigment; the larger the value of K_s, the greater the unit reflectance and therefore the closer the reflectance will approach to an arbitrary maximum. R_∞ in this case has been taken to be 95%. The R_{450} reflectance values of the coatings were measured at 450nm; R_{i-r} was determined as an average over the 700-2600nm region. The formulae for K_{450} and K_{i-r} thus become

$$K_{450} = \ln(1-R_{450}/95)/x \qquad \text{(I-5)}$$

$$K_{i-r} = \ln(1-R_{i-r}/95)/x \qquad \text{(I-6)}$$

The coating weight (m) was used in place of coating thickness, x. Accordingly all the K values will have units of gm^{-1}. To convert to cm^{-1}, the standard unit of absorptance, the coating thickness (x) is required. The area of an IRIF coupon (A) and material density (ρ) are 3.00 cm^2 and 5.07 gm/cm^3, respectively. Thus, the thickness of the film is

$$x = \frac{m}{A\rho} = m/15.21 \qquad \text{(I-7)}$$

The values of K in table consequently should be multiplied by the factor 15.21 to convert them to cm^{-1} units. There are two assumptions, however, which make this conversion somewhat risky. First, it is necessary to assume that the coating is uniform in thickness. Second, the density used above applies to Zn_2TiO_4; it may be more or less for a non-stoichiometric material.

APPENDIX II

Band Edge Properties

The band edge properties appearing in Table 4 were calculated from data taken from the reflectance spectra of the pigments. Figure II-1 shows a typical reflectance spectrum and also the relationships used to calculate the properties and characteristics of the absorption band.

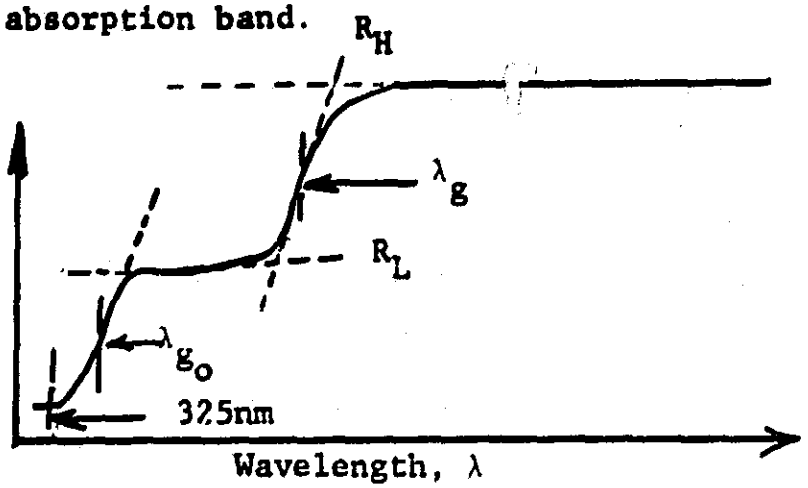


Fig. II-1 BAND EDGE RELATIONSHIPS

The property of primary interest is the value for Zn_2TiO_4 of the fundamental band gap energy, E_{g_o}, which frequently is disguised by impurity absorption with an apparent band edge value of E_g. The value of E_g (in eV) is numerically equal to $1239.7/\lambda_g(nm)$.

The values are calculated in the following way. Tangents are drawn to the visible reflectance and to the "knee" reflectance. Another tangent is drawn to the vertical portion of the spectral reflectance curve. The intersection of the latter tangent with the two previously mentioned tangents defines two points, designated R_H and R_L, with associated wavelengths designated λ_H and λ_L. By convention λ_g is taken as the mean of

λ_H and λ_L, i.e.

$$\lambda_g = 1/2 \cdot (\lambda_H + \lambda_L) \qquad \text{(II-I)}$$

The value of the reflectance at λ_g is designated R_g. This method was used to calculate both E_g, and $E_{.60}$, the latter being applicable only to the spectra of those materials with a relatively high "knee".

APPENDIX III

"TiOx" Analysis and Theoretical Background

The rates at which chemical reactions proceed and the equilibrium conditions they reach can often be analyzed to indicate their nature. In the present case we have a material with an unknown composition ("TiOx"), which when heated sufficiently will reduce to TiO_2, or, if heated with ZnO, will react with it to form Zn_2TiO_4. What actually happens in either case - (chemical reaction-wise) - may in part be deducible from the equilibrium and/or rate constants.

In classical theory the rate at which two reactants, A and B, react to form a product P depends upon two rate constants, one k_1 defined by the forward reaction,

$$A + B \xrightarrow{k_1} P; \qquad \text{(III-1)}$$

and the other, k_2, defined by the reverse reaction,

$$P \xrightarrow{k_2} A + B \qquad \text{(III-2)}$$

The reaction rate constant, K, is predicted by the Arrhenius equation

$$K = k_1/k_2 = S \cdot \exp(-\Delta H/RT), \qquad \text{(III-3)}$$

where

S = a frequency factor (of the order 10^{12}-10^{14} sec-1),
ΔH = heat of activation, cal/mole
R = Universal gas constant (1.987 cal. $mole^{-1}$. $°K^{-1}$)
T = Absolute temperature, °K.

For a first order reaction, the overall reaction rate is:

$$\frac{dc_p}{dt} = -Kc_p \qquad \text{(III-4)}$$

where c_p is the concentration of the product, and t = time. A second order reaction is more complicated (mathematically), but is tractable and analyzable. It appears though that the reactions we are dealing with are first order, with respect to titanium, mainly because the product (either TiO_2 or Zn_2TiO_4) and their common precursor contains one atom of Ti per mole i.e., because one Ti gram-atom in the reactant becomes on Ti gram atom in the product. (With respect to Zn, the reaction of ZnO and TiO_2 to form Zn_2TiO_4 would be second order because it requires 2 gm-atoms of Zn in the reactants to form one gram-mole of product).

Treating the reactions then as first order allows us to expect that the solution to eq. III-4 will be exponential in time, i.e.

$$c_p = \exp(-Kt) \qquad \text{(III-5)}$$

The validity of our approach rests on the definition of parameters available to us in terms of those used in classical thermodynamics. We have defined the fractional completion of a reaction as fraction of the ultimate (equilibrium) concentration. In a typical TGA test (see Fig. 16), the material loses mass continuously until, at some point, further increases in temperature produce no additional mass loss, - in this case, temperatures beyond 500°C. If the ultimate mass loss is such that the product mass is 50% of the reactants' mass, then at any given intermediate time the conversion will, in a first order (linear) reaction, be the instantaneous fractional mass loss divided by 0.5. In more general terms, if the ultimate fractional mass loss is r, (implying 100% conversion of reactants to products or 100% achievement of the maximum possible yield), then the instantaneous (intermediate) fractional conversion is x/r, where x is the instantaneous fractional mass loss.

Yield calculations are accomplished somewhat differently. Referring to TiO_2 yield, the ensuing discussion will establish the basis for determining the yield and for distinguishing it from FML, the overall index of conversion.

The postulated reactions in the calcination of "TiOx" are:

$$Ti(OH)_2CO_3\ 0.5H_2O \xrightarrow{\Delta} Ti(OH)_2CO_3 + 0.5H_2O\uparrow \qquad \text{(III-6)}$$

(150.950) (141.942) (9.008)

$$Ti(OH)_2CO_3 \xrightarrow{\Delta} TiO_2 + CO_2\uparrow + H_2O\uparrow \qquad \text{(III-7)}$$

(141.942) (79.90) (44.0) (18.016)

For H_2O removal (at temperatures below 200°C) we expect the % wt. loss (max.) to be (9.008/150.950)x 100 = 5.967 w/o. In the conversion reaction (at temperatures above ~225°C), we expect the % wt. loss (after H_2O evolution) to be [(18.016 + 44.01)/141.942]x100 = 43.698 w/o. The overall wt. loss, theoretically, should be

(71.05/150.950)x100 = 47.069 w/o.

% wt loss data, therefore, should be corrected by substracting 5.967 w/o. On this basis the ultimate wt. loss must also be corrected, from 47.069 w/o, to 41.102 w/o.

The yield, the percentage conversion of "TiOx" to TiO_2, can be calculated from the percentage weight loss assuming that water evalution is essentially complete prior to any significant conversion of $Ti(OH)_2CO_3$ to TiO_2.

The percentage weight loss, F', is

$$\frac{\text{weight loss}}{\text{initial weight}} \times 100$$

The incomplete reaction may be written as follows:

$$Ti(OH)_2CO_3 \cdot 0.5H_2O \xrightarrow{\Delta} Ti(OH)_2CO_3 \xrightarrow{\Delta} Y \cdot TiO_2 + X \cdot Ti(OH)_2CO_3$$

$$M_o(150.9450) \quad M_1(141.942) \quad M_2(79.90) \; M_1(141.942)$$

This relationship indicates that 1 mole of wet TiOx is calcined to produce 1 mole of dry TiOx, which in turn is calcined to produce Y mole of TiO_2 and X mole of dry (unreduced) TiOx. In a complete reaction Y = 1, and X=0. It then follows that

$$F' = \frac{M_o - (Y \cdot M_2 + X \cdot M_1)}{M_o} \times 100 \qquad \text{(III-8)}$$

Defining F = F'/100, the fractional wt. loss, we can solve for Y which is the fractional TiO_2 yield (on a one-mole basis). The solution is based on the fact that Y + X = 1; thus X=1-Y, and,

$$FM_o = M_o - YM_2 - (1-Y)M_1; \qquad \text{(III-9)}$$

therefore,

$$Y = \frac{M_1 - M_o(1-F)}{M_1 - M_2} \qquad \text{(III-10)}$$

Inserting the appropriate values of M_o, M_1 and M_2 gives the fractional yield:

$$Y = 2.4330 \cdot F - 0.1452 \qquad \text{(III-11)}$$

Dynamic (TGA) and static tests produce comparable but somewhat different results. We have accomplished both. Dynamic tests may or may not allow equilibria to be reached, since equilibrium points are temperature-dependent. Specifically, the TGA data on TiOx are based on a 5°C/min heating rate. Our other mass loss data (from static tests) are based on exposures to high temperatures for much longer periods of time. In static

tests, therefore, the attainment of equilibrium conditions is very much more likely than in the TGA case because of much longer times at temperature.

The Clausius-Clapeyron equation, a different form of the Arrhenius equation, provides a direct means of calculating the energies involved in the calcination reactions. The equation is obtained by differentiating the Arrhenius equation with respect to temperature, and then integrating between temperature limits. The resulting expression is:

$$\log_e K_2 - \log_e K_1 = \log_e (K_2/K_1) = \frac{(\Delta H_A)}{R} \cdot \left(\frac{1}{T_2} - \frac{1}{T_1}\right) \quad \text{(III-6)}$$

The slope of the plot of log K vs (1/T), therefore, is $\Delta H/R$, from which the heat of reaction ΔH may be easily determined. Using the data in Table 8, the heat of activation in the conversion of "TiOx" to TiO_2 can be calculated in the following manner. Taking the data points at 200°C and at 275°C., we can set up the table:

Temp. °C	$10^3/T(°K)$	% Conversion	Y	$\log_{10} Y$
200	2.114	10.60	.1127	-0.9480
275	1.825	31.80	.6285	-0.2018

Inserting these data in the Clausius - Clapeyron equation gives

$$(2.303)\ (-0.9480-0.2017) = \frac{\Delta H_A}{1.987}(2.114-1.825)\times 10^{-3}$$

$$\Delta H_A = -\ 11817 \text{ cal/mole}$$

This value pertains to H_2O evalution. For the high temperature region we can utilize the 340°C and 500°C static data from table 6 to obtain

Temp, °C	$10^3/T(°k)$	%Conversion	Y	$\log_{10} Y$
325	1.672	41.7	.8217	-.08530
400	1.486	44.7	.9424	-.02577

Proceeding as above, we obtain 1464 cal/mole. A better value in both the high and low temperature regions can be obtained from smoothing the plotted data. The values reported in the text are smoothed values based on best-fit of the data in Fig. 17.

4. COMPREHENSIVE REVIEW

4.1 Introductory Remarks

Since the inception of this program a vast amount of data has been accumulated regarding the solar absorptance (α_s) and solar ultraviolet radiation stability ($\Delta\alpha_s$) of developmental pigments. The variables associated with the oxalate precursor method in general are so numerous and complex that the effect of any single one would be nearly impossible to measure; this is especially true in comparing results from one test to another, since each of the many irradiation tests had individualized objectives and few had common ones. An effort was initiated to identify the important process parameters, materials variables and treatment conditions affecting α_s and $\Delta\alpha_s$. Though the tables which follow are far from complete, they do indicate some important trends and, to the maximum extent possible, the important indices of pigment properties and environmental performance.

4.2 Indices of Performance

The indices of environmental stability, $\Delta\alpha_s$, are ΔR_{400} and ΔR_{900}. ΔR_{900} measures degradation in the pigment, while ΔR_{400} is a response associated principally, but not necessarily entirely, with the silicone binder. The optical response of a paint to ultraviolet irradiation consists of decreases in spectral reflectance attributable to increased spectral absorption in the pigment and in the binder. For zinc orthotitanate it is not unusual that the binder "sensitizes" the pigment, causing markedly greater degradation at 900nm than the pigment sustains when irradiated as a powder. To a lesser but still noticeable extent, the pigment - presumably because of surface defect sites - also sensitizes the silicone binder causing it to degrade more than if it were unpigmented. The synergism

becomes quite apparent in comparing the ΔR_{400} and ΔR_{900} values of OI650 paints with those of the pigments alone; quite frequently the pigment/vehicle "damage" ratio, $\Delta R_{900}/\Delta R_{400}$, of the paint will greatly differ from that of the pigment. The effectiveness of surface treatments can be assessed in terms of reduced values of ΔR_{900} and ΔR_{400} - but, unfortunately, only within rather narrow limits. The A-10 treatment, for example, appears to aid some pigments while not affecting others; on the other hand, it does not have any serious adverse effects. Of the various encapsulants K_2SiF_6 offers pigment surface protection in more cases than do others, although it is not intrinsically superior to others.

The very large number of factors affecting α_s and $\Delta\alpha_s$ and the complex interrelationships between them make it especially difficult to construct any but the most generalized expressions relating α_s and $\Delta\alpha_s$ to those factors. The study nevertheless has been very valuable in identifying factors which had heretofore been unsuspected or uncontrolled. The differences in properties and perfo.mance between materials in many cases must be ascribed to coating charactersitics (thickness, etc.) and to batch-to-batch variations: batch size(s), temperature, and other precipitation conditions, stoichiometry variations, human errors, etc. The relative importance of several factors can be determined in many cases by inspection of the data; in others, it must be discerned by carefully designed and interpreted tests. The effect of time, for example, is probably a primary factor in the precipitation process but in most other instances it is of second-order importance. Temperature, of course, is of prime importance in the calcination process. The intent of the review included the determination of those factors to which α_s and $\Delta\alpha_s$ are most sensitive. The operation of several factors, not all acting in the same direction, has disguised the true importance of any of them, individually. The importance of

calcination temperature is easily discernible from theory and experience, but in certain instances its effects are made less pronounced, for example, by batch-to-batch variations, or by different irradiation test conditions. Table 9 summarizes the more important considerations and presents a listing of the more important factors affecting α_s and $\Delta\alpha_s$.

Table 9

Critical Property/Performance Relationships

Index	Dependence Factors
R_k	Free ZnO or TiO_2 or other strong near UV absorbers will decrease reflectance below 380nm in proportion to amount present.
R_{400}	Pigment particle size (d_p) and packing density, coating thickness, binder indices of refraction, and PVC.
d_p	Precursor particle size(s), calcination conditions (temperature and time), precipitation conditions, size reduction effectiveness.
R_{max}	Binder index of refraction and d_p.
λ_{max}	Peak reflectance relates to predominant effective particle size and to ratio of refractive indices of pigment to binder; breadth of maximum depends on particle size range.
α_s	$\int_0^\infty R_\lambda . S_\lambda . d\lambda / \int_0^\infty S_\lambda . d\lambda$
$\Delta\alpha_s$	α_s (after irradiation) - α_s (initial)

Table 9 (Cont'd)

Critical Property/Performance Relationships

Index	Dependence Factors
ΔR_{400}	Bulk effects of radiation on binder (induced) absorption and pigment (induced) absorption; relates to number density of intrinsic or potential defects.
ΔR_{900}	Area number density of surface defects - total number, dependent on particle surface area; surface density, dependent upon preparative and/or treatment conditions.
$\Delta R_{2.6}$	(very uncommon). Free carrier effect (usually); directly related to volume number density of free ZnO molecules. $\Delta R_{2.6} \propto N^*_{2.6} \cdot \lambda^3$ where $N^*_{2.6}$ is the area number density of ZnO molecules in which O^- has been photo-desorbed.

We have attempted to determine the effects of various preparative conditions, environmental influences, etc. upon the reflectance at specific wavelengths. Thus the value of α_s is primarily sensitive to the value of R_{max} and its spectral location, and also to the value of R_k(370nm). The higher the value of R_{max}, the lower will be the value of α_s, and, obviously, α_s will be further improved if the location of maximum reflectance occurs at or near the peak of the solar energy intensity spectrum. The value of R_k is determined by the UV reflectance in the region between 350nm and 400nm. It can make the difference between a paint with $\alpha_s = 0.15$ and one with $\alpha_s = 0.08$. R_k otherwise, is not particularly important - at least not in terms of α_s.

4.3 Analyses

It would be far too cumbersome to describe and present all of the attempts to correlate pigment properties and environmental performance with the many factors which affect them. More importantly, the MOX-A findings strongly affect these correlation attempts. Initially, for example, we were concerned with the effect of minor variations in the initial Zn/Ti ratio on α_s and on $\Delta\alpha_s$; the MOX-A results indicated an improvement (decrease) in α_s but a substantial penalty (increase) in $\Delta\alpha_s$. This conclusion is borne out to some extent by concurrent plots of α_s and $\Delta\alpha_s$ vs R_k. Referring to table 10, even a casual study of the data shows that a correlation between properties and performance is unlikely because of the lack of any specific trend(s). Important relationships such as α_s and $\Delta\alpha_s$ vs calcination conditions (temperature and time) likewise show very little correlation ∞ which is consistent from test to test.

4.4 Conclusions

As we noted specific relationships between α_s, $\Delta\alpha_s$ and the important factors affecting them remain very difficult to establish, mainly because a large number of factors act concurrently and their effects frequently are synergistic, in nonmutual directions, and with numerous side-effects. Based on a thorough study of the data in table 10 and a considerable amount of back-up data the choice of base-line pigments remains as 6-12 and 6-12-A-10.

In general degradation is always higher in a paint system than in the pigment alone; the influence of the binder on pigment degradation (ΔR_{900}) is almost always greater than the effect of pigment on binder degradation (ΔR_{400}). Even though the nature of the surface defects in Zn_2TiO_4 is uncertain, their

relative optical effect and the effectiveness of various treatments in passivating them can be assessed by the ΔR_{900} data, especially those obtained from post irradiation oxygen bleach reflectance spectra. The A-10 treatment, on the basis of O_2 adsorbate data, seems most effective, particularly at lower calcination temperatures which produce finer particles with more surface (and thus with better free ZnO removal potential). The choice of encapsulant, if one must be made, would be K_2SiF_6.

The data on MOX-A and MOX-C through MOX-G series pigments, irradiation test results of MOX-A pigments and paints, and related information prove beyond any reasonable doubt that pigment stoichiometry critically affects both α_s and $\Delta\alpha_s$ and that the most useful and stable pigment should be one with exact Zn_2TiO_4 stoichiometry. Even though a greater number of surface defects would be anticipated in smaller particles, little, if any, clear evidence exists that ΔR_{900} increases as a result, thus justifying efforts to reduce the particle size of the Zn_2TiO_4 pigment. Particle size studies and reflectance data consistently show that Zn_2TiO_4 paints hold a very realistic possibility of achieving $\alpha_s \leq .10$ and of realizing minimal degradation ($\leq .05$ in 10^4 ESH).

Table 10

Comprehensive Listing of Zinc Orthotitanate Pigments and Paints

Introductory Remarks

This table lists most, if not all, of the Zn_2TiO_4 pigments and paints produced and tested during the current program and summarizes much of the pertinent data. The identification of the pigments follows the code consistently used in the past. With the exception of a few prepared by the solid state (SS) process, all of the pigments have been prepared from oxalate precursors, either by the co-precipitation (COP) method or by the mixed-oxalate ("MOX") method. Paints are distinguished from pigment powders by the designation /OI or /G following the pigment description; OI refers to Owens Illinois 650 "Glass Resin" silicone binder, and G refers to the IITRI-modified version of OI-650. R_k is the initial value of the diffuse spectral reflectance at 370nm; R_{400}, that at 400nm, and R_k/R_{400} is the ratio of these values. R_{max} and λ_{max} refers to the value of the highest diffuse spectral reflectance and to the wavelength(s) or wavelength region(s) at which it is a maximum. Particle size indicates the average size (in microns) of the pigment as determined from SEM photomicrographs. The notations N, MN, SN, Ag, and SM in the particle size column refer to the necking of particles: medium necking, strong necking, agglomerate and submicron. ΔR_{400} and ΔR_{900} values refer to the difference between the initial and post-irradiation spectral diffuse reflectance values at 400nm and at 900nm, respectively; a value following a / indicates this same difference after a post-irradiation oxygen bleach. The other data - ESH, α_s and $\Delta\alpha_s$ - have, of course, the usual meaning.

Table 10A- 1400°C Pigments (And Their Paints)

Sample No.	Description*	$R_{k(\%)}$	R_k/R_{400}	$R_{max(\%)}$	$(\lambda_{max})\mu$	Particle Size, μ	ΔR_{400}	ΔR_{900}	ESH	Initial a_s	Δa_s
C-10-10	LH-12(6-14)	56		89	0.45-0.66	2-6SN	0.01	0.23	1468	.162	.162
C-10-12	LH-16(6-14)	21		89	0.48-0.58	- SN	0.01	0.05	1468	.193	.053
C-10-6	LH-20(9-14)	73		93	0.39-0.47	1-5SN	0.04	0.03	1468	.169	.007
C-10-5	LH-22(9-14)	34		91	1.58-1.9	1-5SN	0.00	0.01	1468	.196	.024
C-10-7	LH-27(9-14)	50		90-96	1.0 -2.6	1-5SN	0.04	0.05	1468	.166	.043
I-60-4	LH-30(6-14)/G(A-37)	57		78	0.5	1.5	0.07	0.15	1096	-	-
I-60-5	LH-30(6-14)/G	56		78	0.46-0.58	1-5	0.05	0.12	1096	-	-
I-60-1	LH-31(6-14)/G	68		78	0.5-0.6	1-5	0.07	0.10	1096	-	-
I-60-3	LH-31(6-14)/G	68		79	0.52-0.55	1-5	0.07	0.10	1096	-	-
C-13-12	LH-51(6-14)/G	84		84	0.36-0.38	2-5SN	0.07	0.05	2106	.149	.069
C-13-11	LH-51(6-14) B/G	82		83	0.36-0.37	2-5SN	0.07	0.04	2106	.157	.072
I-67-1	LH-52(6-14)/OI	50	.65	87	(0.4-0.5)	2.5SN	.06	.22	2050	.250	.120
I-67-2	LH-52(6-14-A-10)/OI	51	.67	80	(0.4-0.5)	2-5SN	.035	.10	2050	.309	.055
C-13-1	LH-30(6-14-A-10)/G	82		86	0.4-0.44	2-5SN	0.04	0.07	2106	.234	.045
C-13-6	LH-30(6-14-A-10)B/G	89.5		89.5	0.34-0.36	2-5SN	0.05	0.02	2106	.212	.044
C-13-2	LH-31(6-14-A-10)/G	91		92	0.34-0.37	2-5SN	0.10	0.07	2106	.184	.098
C-13-8	LH-31(6-14-A-10)B/G	91		82	0.35	2-5SN	0.08	0.06	2106	.189	.081

Table 10B- 1300°C Pigments (And Their Paints)

I-67-10	LH-53(6-13)/OI	54	.69	87	(0.4-0.5)	-	.055	.185	2050	.249	.105
I-67-3	LH-53(6-13-A-10)/OI	62	.83	79	(0.4-0.5)	-	.045	.085	2050	.304	.048

Table 10C - 1250°C Pigments

Sample No.	Description*	$R_{k(\%)}$	R_k/R_{400}	$R_{max(\%)}$	$(\lambda_{max})\mu$	Particle Size, μ	ΔR_{400}	ΔR_{900}	ESH	Initial α_s	$\Delta\alpha_s$
I-68-6	(SS)T-4	32	.51	84	(2.6)		.031	.026	370	-	-
I-69-11	(SS)T-4(A-10)	55.0	.77	90.0	(2.1,2.6)		.13	.01	2600	.224	.079

Table 10D - 1200°C Pigments (And Their Paints)

I-72-12	MOX-B(6-12/2)	51	.61	93	(0.45-575)	1-5SN	.055	.070	2630	.141	.049
I-71-2.	MOX-A(6-12/0.5)	81.5	.94	97	(2.0,2.6)	1-5Ag+N	.05	.12	460	.116	.068
I-71-11	MOX-A(6-12/2)	80.5	.94	97.5	(2.6)	1-5Ag+N	.025	.055	460	.114	.032
C-10-4	LH-20(6-12)	67		92	0.44-0.54	1-5MN	0.04	0.04	1468	.146	.011
C-10-3	LH-22(6-12)	32		91	0.46-0.55	2-5MN	0.02	0.07	1468	.173	.047
C-10-1	LH-26(6-12)	57		90	0.50-0.6	-MN	0.00	0.01	1468	.178	.008
C-10-2	LH-27(6-12)	46		(89)	(0.43-0.48)	-MN	0.04	0.08	1468	.201	.035
C-9-9	LH-12(12/1)	-		(Sample Destroyed During Test)						0.278	-
I-68-5	(SS)T-3	38	.55	83 85	(0.5-0.6) (2.6)		.029	.049	370	-	-
I-69-12	(SS)T-3(A-10)	66.0	.87	84.9	(1.5,1.6)		.16	.02	2600	.210	.051
C-9-5	C-411(9.25/18):K_2SiF_6 (Recalcine 12/16)	71	.85	91	0.43-0.48		0.10	0.04	4070	0.1580	
I-69-3	(SS)T-3/OI	72.0	.46	79.5	(1.8,2.0)		.05	.05	2600	.318	.027
I-60-9	LH-30(6-12)/G	45		72	0.60-0.62	1-5	0.05	0.06	1096	-	-
I-60-11	LH-30(6-12)/G	45		72	0.60		0.04	0.08	1096	-	-
I-60-8	LH-31(6-12)/G	63		73	0.60-0.62	1-5	0.06	0.07	1096	-	-
I-60-10	LH-31(6-12)/G(A-37)	61		73	0.61-0.62	1-5	0.07	0.09	1096	-	-
C-13-10	LH-51(6-12)/G	80		80	0.34-0.37	2-5MN	0.07	0.04	2106	.278	.066
C-13-9	LH-51(6-12)B/G	79		79	0.34-0.38	2-5MN	0.07	0.07	2106	.278	.070
I-67-5	LH-53(6-12)/OI	53	.64	86	(0.4-0.5)	2-5MN	.04	.115	2050	.262	.063

Table 10D - (Cont'd)

Sample No.	Description*	R_k(%)	R_k/R_{400}	R_{max}(%)	$(\lambda_{max})\mu$	Particle Size, μ	ΔR_{400}*	ΔR_{900}*	ESH	Initial α_s	$\Delta\alpha_s$
I-69-4	LH-53(6-12)/G	45.0	.72	67.0	(1.8,1.9)	2-5	.15	.04	2600	.391	.038
C-15-4	LH-102(6-12)/G	61	.81	92	1.9-2.1	2-5MN	.08/.09	.065.025	2190	.183	.047
C-15-5	LH-102(6-12-10)/G	64	.87	85	1.9-2.1	2-5MN	.06/.08	.05/.005	2190	.226	.046
C-15-9	LH-103(6-12)/G	23	.31	88	1.9-2.1	2-5MN	.05/.05	.04/.025	2190	.219	.027
I-70-2	LH-106(6-12-10)/G	75	.91	90	(1.8-2.1)	2-5MN	.045	.06	3132	.180	.034
I-72-7	MOX-B(6-12/0.5)/G	37.5	.53	86	(.57-.62)	1-5SN	.070	.130	2630	.228	.074
I-72-8	MOX-B(6-12/2)/G	34	.54	87	(.47-0.6)	1-5SN	.050	.095	2630	.216	.060
I-69-1	(SS)T-3(A-10)/OI	62.0	.90	74.0	(1.8,2.0)		.09	.06	2600	.319	.043
C-13-4	LH-30(6-12-A-10)/G	82		83	0.34-0.35	2-5MN	0.08	0.06	2106	.259	.077
C-13-7	LH-30(6-12-A-10)/B	81		81	0.34-0.36	2-5MN	0.04	0.02	2106	.270	.034
C-13-3	LH-31(6-12-A-10)/G	83		86	0.34-0.35	2-5MN	0.07	0.04	2106	.252	.067
C-13-5	LH-31(6-12-A-10)B/G	86		87	0.34-0.36	2-5MN	0.09	0.08	1206	.227	.084
I-67-9	LH-53(6-12-A-10)/OI	78	.93	84	(0.4-0.5)	2-5MN	.06	.125	2050	.259	.071
C-15-6	LH-102(6-12-A)/G	55.5	.90	84	1.9-2.1	2-5MN	.08/.04	.185/.005	2190	.272	.117
C-15-7	LH-102(6-12-A-10)/G	69	.91	89	1.9-2.1	2-5MN	.045/.03	.02/.005	2190	.214	.016
I-70-1	LH-106(6-12)/G	75	.90	93	(1.7-1.8)	2-5MN	.04	.065	3132	.152	.019
C-16-6	LH-106(6-12-A-10)/G	72.5	.91	89	1.9-2.1	2-5MN	.14	.05/.015	4720	.182	.064
I-70-3	LH-106(6-12-A-10)/G	72	.91	86	(1.9-2.0)	2-5MN	.025	.065	3132	.213	.030
C-8-5	(K_2SiF_6)recal. (12/.16)/OI	94		94	0.36-0.38		0.04	0.01	1000	.152	.042
C-8-3	(K_2SiF_6)recal. (12/.16)/OI	86		86	0.36-0.38		0.1?	0.03	1000	.245	.101
C-8-8	(K_2SiF_6)recal. (12/.16)/OI	85		86	0.35-0.36		0.10	0.02	1000	.244	.088

Table 10D- (Cont'd)

Sample No.	Description*	R_k(%)	R_k/R_{400}	R_{max}(%)	$(\lambda_{max})\mu$	Particle Size, μ	ΔR_{400}	ΔR_{900}	ESH	Initial α_s	$\Delta\alpha_s$
C-9-7	K_2SiF_6(12/.16)/G	57		83	0.43-0.45		0.10	0.01	4070	.253	.045
C-9-6	K_2SiF_6(12/.16)/OI	56		88	0.43-0.54		0.08	0.14	4070	.216	.093
I-70-10	LH-106(6-12): K_2SiF_6/G	73.5	.92	88	(1.8-2.0)	2-5MN	.03	.03	3132	.192	.021
C-16-11	LH-106(6-12): K_2SiF_6/G	73.0	.92	89	1.9-2.1	2-5MN	.08	.055/.02	4720	.208	.059
I-70-11	LH-106(6-12-10): K_2SiF_6/G	73.5	.94	85	(1.8-2.0)	2-5MN	.03	.025	3132	.215	.016
C-16-12	LH-106(6-12-10): K_2SiF_6/G	71.5	.92	88	1.9-2.1	2-5MN	.095	.025/.055	4720	.226	.040
I-70-12	LH-106(6-12-A-10): K_2SiF_6/G	73.5	.94	89	(1.8-2.0)	2-5MN	.035	.09	3132	.206	.028
C-15-1	LH-102(6-12): Li_2SiO_3/G	64.5	.87	90	1.9-2.1	2-5MN	.09/.095	.065/.015	2190	.193	.045
C-15-10	LH-102(6-12-A): Li_2SiO_3/G	59	.82	87	1.9-2.1	2-5MN	.19/.12	.335/.03	2190	.229	.205
C-15-2	LH-102(6-12-10): Li_2SiO_3/G	68.5	.90	89	1.9-2.1	2-5MN	.16/.165	.05/.02	2190	.217	.047
C-15-3	LH-102(6-12-A-10): Li_2SiO_3/G	59.5	.77	86	1.9-2.1	2-5MN	.16/.16	.035/.00	2190	.224	.038
C-15-8	LH-103(6-12): Li_2SiO_3/G	38	.51	90	1.9-2.1	2-5MN	.04/.05	.025/.01	2190	.209	.042
I-70-4	LH-106(6-12): Li_2SiO_3/G	72	.92	86	(1.8-2.0)	2-5MN	.03	.05	3132	.203	.021

Table 10D-(Cont'd)

Sample No.	Description*	R_k(%)	R_k/R_{400}	R_{max}(%)	$(\lambda_{max})\mu$	Particle Size, μ	ΔR_{400}	ΔR_{900}	ESH	Initial α_s	$\Delta\alpha_s$
C-16-7	LH-106(6-12): Li_2SiO_3/G	72.5	.91	86	1.9-2.1	2-5MN	.115	.05/.02	4720	.208	.043
I-70-5	LH-106(6-12-10): Li_2SiO_4/G	74	.93	88	(1.8-2.0)	2-5MN	.03	.025	3132	.194	.018
C-16-8	LH-106(6-12-10): Li_2SiO_3/G	74.0	.91	90	1.9-2.1	2-5MN	.125	.03/.04	4720	.181	.043
C-16-9	LH-106(6-12-A-10): Li_2SiO_3/G	73.0	.91	88	1.9-2.1	2-5MN	.095	.02/.04	4720	.217	.028
I-70-6	LH-106(6-12-A-10): Li_2SiO_3/G	74.5	.93	88	(1.8-2.0)	2-5MN	.03	.02	3132	.180	.014
I-69-2	T-3:K_2SiO_3/OI	66.0	.87	74.0	(0.7,0.8)		.06	.04	2600	.372	.026
C-16-10	LH-106(6-12):K_2SiO_3/G	73.0	.92	84	1.9-2.1	2-5MN	.12	.05/.025	4720	.224	.043
I-70-7	LH-106(6-12):K_2SiO_3/G	73.5	.94	82	(1.8-2.0)	2-5MN	.025	.02	3132	.232	.012
I-70-8	LH-106(6-12-10): K_2SiO_3/G	73	.92	88	(1.8-2.0)	2-5MN	.025	.02	3132	.187	.016
C-16-5	LH-106(6-12-A-10): K_2SiO_4/G	76.5	.83	88	1.9-2.1	2-5MN	.155	.05/.01	4720	.197	.056
I-70-9	LH-106(6-12-A-10): K_2SiO_3/G	76.5	.94	85	(1.8-2.0)	2-5MN	.025	.02	3132	.210	.015
C-8-2	($PO_4/SiO_3/PO_4$)recal. (12/.16)/OI	90		90	0.37-0.38		0.18	0.07	1000	.214	.185
C-8-7	($PO_4/SiO_3/PO_4$)recal. (12/.16)/OI	88		88	0.35-0.36		0.16	0.04	1000	.242	.151

Table 10D - (Cont'd)

Sample No.	Description*	R_k(%)	R_k/R_{400}	R_{max}(%)	$(\lambda_{max})\mu$	Particle Size, μ	ΔR_{400}	ΔR_{900}	ESH	Initial α_s	$\Delta\alpha_s$
C-8-11	Zn_2TiO_4(9.25/18) (Li_2SiF_6)recal. (12/.16)/OI	82		84(85)	0.4-0.42		0.09	0.03	1000	.175	.084

Table 10E - 1100°C Pigments

I-67-6	LH-53(6-11)/OI	64	.74	87	(0.3-0.5)	1-5N	.035	.09	2050	.220	.051
I-67-4	LH-53(6-11-A-10)/OI	77.5	.84	83	(0.4-0.5)	1-5N	.055	.115	2050	.286	.064

Tabl 10F - 1050°C Pigments

I-72-10	MOX(6-10.5/2) Powder	57	.62	96	(0.45-.47)	0.5-2	.030	.031	2630	.111	.023
I-71-6	MOX(6-10.5/2)	56	.65	93	(1.7,2.0)	0.5-2	.02	.02	460	.132	.006
I-71-9	MOX-A(6-10.5/2)	71	.85	98	(2.6)	1-4Ag	.035	.055	460	.124	.034
I-71-10	MOX-A(6-10.5/4)	69	.85	97.5	(2.6)	1-4Ag	.02	.055	460	.143	.030
I-71-5	MOX-A(6-10.5/8)	72	.89	90.5	(2.6)	1-4Ag	.05	.085	460	.160	.049
I-72-11	MOX-B(6-10.5/8)	56	.68	86	(0.44-0.5)	1-5Ag+N	.040	.032	2630	.207	.030
I-71-3	LH-103(6-10.5/2)	39	.47	90.5	(0.5,0.6)	1-5N	.03	.065	460	.165	.033
I-71-4	LH-103(C6-10.5/2)	41.5	.49	91	(0.5,0.6)	1-5N	.025	.04	460	.160	.022
I-72-4	MOX-B(6-10.5/1)/G	33.5	.47	89	(0.6-62)	1-5Ag+N	.115	.182	2630	.204	.111
I-72-5	MOX-B(6-10.5/4)/G	36	.51	88	(.57-0.6)	1-5Ag+N	.082	.169	2630	.212	.098
I-72-6	MOX-B(6-10.5/8)/G	36	.50	87.5	(.57-0.6)	1-5Ag+N	.089	.125	2630	.214	.065

C6233-48

Table 10G- 900°C Pigments (And Their Paints)

Sample No.	Description*	R_k(%)	R_k/R_{400}	R_{max}(%)	$(\lambda_{max})\mu$	Particle Size, μ	ΔR_{400}	ΔR_{900}	ESH	Initial d_s	$\Delta\alpha_s$
C-9-2	(9.25/18)	49		98	0.43-0.47		0.07	0.04	4070	.114	.060
I-68-8	(SS)T-2	43	.52	91	(2.6)		0.058	.026	370	-	-
I-69-10	(SS)T-2	42.5	.56	90.0	(0.7)		.15	.01	2600	.187	.113
C-9-10	LH-12(900/8)	27		93	0.43-0.51		0.06	0.09	2010	.173	-
C-9-8	LH-14(900/8)	36		95(95)	0.53-0.58(0.76-0.84)		0.00	0.10	4070	.142	.127
C-10-9	LH-16(9)	31		95	0.45-0.5		0.02	0.04	1468	.130	
C-10-8	LH-20(9)	70		96	0.4-0.45	SM-3	0.04	0.03	1468	.116	.020
C-10-11	LH-22(9)	35		96	0.43-0.6	SM-4	0.04	0.04	1468	.141	.028
I-67-11	LH-52(6-9)	71	.93	95	(0.4-0.5)	SM-5 R	.03	.03	2050	.156	.017
I-71-7	MOX-A(6-9/4)	63	.81	91	(2.6)	1-3	.03	.05	460	.170	.024
I-71-8	MOX-A(6-9/16)	69.5	.84	93	(2.6)	1-3N	.02	.045	460	.157	.016
I-72-9	MOX-B(6-9/16)	55.5	.63	90	(.45-0.52)	SM-3Ag	.045	.040	2630	.174	.026
C-9-11	(9.25/18): $(PO_4/SiO_3/PO_4)$	72		93	0.42-0.47		0.14	.001	4070	.150	.040
I-69-9	(SS)T-2:K_2SiO_3	45.5	.55	91.0	(1.8,1.9)		.105	.02	2600	.166	.030
C-9-3	(9.25/18)/PS7	46		94	0.42-0.51		0.07	0.00	4070	.164	.031
C-9-4	(9.25/18)/OI-650	39		95	0.42-0.46		0.04	0.05	4070	.171	.036
I-60-12	(9.25/18)/G	65		84	0.63-0.65	1-5	0.11	0.06	1096	-	-
I-60-7	(9.25/18)/G(A-37)	63		85	0.60-0.62	1.5	0.11	0.06	1096	-	-
I-69-8	(SS)T-2/OI	37.0	.44		(0.6,0.7)		.125	.02	2600	.187	.049
I-69-5	(SS)T-2/G	33.0	.37		(0.68,0.7)		.07	.03	2600	.136	.022
I-67-7	LH-22(9)/OI	37	.42	92	(0.4-0.5)	-	.02	.07	2050	.24	.05
I-67-8	LH-52(6-9)/OI	43	.57	83	(0.4-0.5)	SM-5R	.04	.15	2050	.287	.083

C6233-48

Table 10G - (Cont'd)

Sample No.	Description*	R_k(%)	R_k/R_{400}	R_{max}(%)	$(\lambda_{max})\mu$	Particle Size, μ	ΔR_{400}	ΔR_{900}	ESH	Initial α_s	$\Delta\alpha_s$
I-72-2	MOX-B(6-9/4)/G	32.5	.49	85	(0.55-0.6)	Sm-3Ag	.130	.230	2630	.235	.127
I-72-3	MOX-B(6-9/16)/G	32	.44	89	(0.7-1.0)	SM-3Ag	.130	.224	2630	.198	.138
C-8-4	(9.25/18):(K_2SiF_6)/OI	93		93	0.35-0.38		0.11	0.02	1000	.171	.057
C-8-9	(9.25/18):(K_2SiF_6)/OI	96		97	0.35-0.36		0.08	0.01	1000	.143	.082
C-8-1	(9.25/18):($PO_4/SiO_3/PO_4$)/OI	97		97	0.36-0.38		0.12	0.03	1000	.134	.091
C-9-12	(9.25/18):($PO_4/SiO_3/PO_4$)/OI	67		95	0.42-0.51		0.07	0.07	4070	.14	.068
C-8-6	(9.25/18):($PO_4/SiO_3/PO_4$)/OI	96		96	0.35-0.37		0.05	0.01	1000	.154	.037
I-60-6	(9.25/18):(PO_4/K-Sil/PO_4)/G	68		84	0.60-0.62	1-5	0.10	0.03	1096	-	-
I-60-2	(9.25/18):(PO_4/K-Sil/PO_4)/G	67		84	0.65-0.7	1-5	0.14	0.05	1096	-	-
C-8-10	(9.25/18):(Li_2SiF_6)/OI	87		89(89)	0.4(0.74)		0.08	0.01	1000	.143	.059
I-69-7	(SS)T-2(A-10)/OI	73.5	.93	89.9	(0.7,0.8)		.09	.015	2600	.233	.034
I-69-6	(SS)T-2:K_2SiO_3/G	35.0	.39	94.0	(0.6,0.7)	.09	.09	.01	1750	-	.082

ORIGINAL PAGE IS OF POOR QUALITY

5. REFERENCES

1. S.F. Bartram and R.A. Slepetys, J. Am. Ceram. Soc. 44, (10), pp. 493-88, 1960.

2. J.E. Gilligan and Y. Harada, "Development of Space-Stable Thermal Control Coatings for Use on Large Space Vehicles," IITRI Report No. C6233-44 (Triannual) Oct. 1974.

3. N.A. Lange, "Handbook of Chemistry," 6th Ed., Handbook Publishers, Inc., Sandusky, Ohio, 1946; CRC Handbook of Physics and Chemistry", 50th Edition, R.C. Weast, (Ed.); Publ., Chemical Rubber Co., Cleveland, Ohio, 1969.

4. S.F.W. Grundall, "A Process for Preparing Basic Titanic Oxalate", U.S. Patent No. 2,027,812, Jan. 1936.